Journal Pre-proofs

Differential early subcortical involvement in genetic FTD within the GENFI cohort

Martina Bocchetta, Emily G. Todd, Georgia Peakman, David M. Cash, Rhian S. Convery, Lucy L. Russell, David L. Thomas, Juan Eugenio Iglesias, John C. van Swieten, Lize C. Jiskoot, Harro Seelaar, Barbara Borroni, Daniela Galimberti, Raquel Sanchez-Valle, Robert Laforce, Fermin Moreno, Matthis Synofzik, Caroline Graff, Mario Masellis, Maria Carmela Tartaglia, James B. Rowe, Rik Vandenberghe, Elizabeth Finger, Fabrizio Tagliavini, Alexandre de Mendonça, Isabel Santana, Chris R. Butler, Simon Ducharme, Alexander Gerhard, Adrian Danek, Johannes Levin, Markus Otto, Sandro Sorbi, Isabelle Le Ber, Florence Pasquier, Jonathan D. Rohrer

PII: S2213-1582(21)00090-5
DOI: https://doi.org/10.1016/j.nicl.2021.102646
Reference: YNICL 102646

To appear in: *NeuroImage: Clinical*

Received Date: 12 January 2021
Revised Date: 8 March 2021
Accepted Date: 23 March 2021

Please cite this article as: M. Bocchetta, E.G. Todd, G. Peakman, D.M. Cash, R.S. Convery, L.L. Russell, D.L. Thomas, J. Eugenio Iglesias, J.C. van Swieten, L.C. Jiskoot, H. Seelaar, B. Borroni, D. Galimberti, R. Sanchez-Valle, R. Laforce, F. Moreno, M. Synofzik, C. Graff, M. Masellis, M. Carmela Tartaglia, J.B. Rowe, R. Vandenberghe, E. Finger, F. Tagliavini, A. de Mendonça, I. Santana, C.R. Butler, S. Ducharme, A. Gerhard, A. Danek, J. Levin, M. Otto, S. Sorbi, I. Le Ber, F. Pasquier, J.D. Rohrer, Differential early subcortical involvement in genetic FTD within the GENFI cohort, *NeuroImage: Clinical* (2021), doi: https://doi.org/10.1016/j.nicl.2021.102646

Differential early subcortical involvement in genetic FTD within the GENFI cohort

Martina Bocchetta PhD[1], Emily G. Todd MRes[1], Georgia Peakman MSc[1], David M. Cash PhD[1,2], Rhian S. Convery MSc[1], Lucy L. Russell PhD[1], David L. Thomas PhD[1,3], Juan Eugenio Iglesias PhD[2,4,5], John C. van Swieten MD PhD[6], Lize C. Jiskoot PhD[6], Harro Seelaar MD PhD[6], Barbara Borroni MD[7], Daniela Galimberti PhD[8,9], Raquel Sanchez-Valle PhD[10], Robert Laforce Jr MD PhD[11], Fermin Moreno MD PhD[12], Matthis Synofzik MD[13], Caroline Graff MD PhD[14,15], Mario Masellis MD PhD[16], Maria Carmela Tartaglia MD[17], James B. Rowe FRCP PhD[18], Rik Vandenberghe MD PhD[19], Elizabeth Finger MD[20], Fabrizio Tagliavini MD[21], Alexandre de Mendonça MD PhD[22], Isabel Santana MD PhD[23], Chris R. Butler FRCP PhD[24], Simon Ducharme MD[25], Alexander Gerhard MRCP MD[26,27], Adrian Danek MD[28], Johannes Levin MD[28], Markus Otto MD[29], Sandro Sorbi MD[30], Isabelle Le Ber MD PhD[31,32,33], Florence Pasquier MD PhD[34,35,36], Jonathan D. Rohrer FRCP PhD[1] on behalf of the Genetic Frontotemporal dementia Initiative (GENFI)*

Affiliations:

[1]Dementia Research Centre, Department of Neurodegenerative Disease, UCL Queen Square Institute of Neurology, University College London, London, United Kingdom

[2]Centre for Medical Image Computing, Department of Medical Physics and Biomedical Engineering, University College London, London, United Kingdom

[3]Neuroradiological Academic Unit, UCL Queen Square Institute of Neurology, University College London, London, United Kingdom

[4]Martinos Center for Biomedical Imaging, Massachusetts General Hospital and Harvard Medical School, USA

[5]Computer Science and Artificial Intelligence Laboratory, Massachusetts Institute of Technology, USA

[6]Department of Neurology and Alzheimer center, Erasmus Medical Center Rotterdam, the Netherlands

[7]Centre for Neurodegenerative Disorders, Neurology Unit, Department of Clinical and Experimental Sciences, University of Brescia, Brescia, Italy

[8]Department of Biomedical, Surgical and Dental Sciences, University of Milan, Milan, Italy

[9]Fondazione IRCCS Ca' Granda, Ospedale Maggiore Policlinico, Milan, Italy

[10]Neurology Department, Hospital Clinic, Institut d'Investigacions Biomèdiques, Barcelona, Spain

[11]Clinique Interdisciplinaire de Mémoire, Département des Sciences Neurologiques, CHU de Québec, Faculté de Médecine, Université Laval, Québec, Canada

[12]Hospital Universitario Donostia, San Sebastian, Spain

[13]Department of Cognitive Neurology, Center for Neurology, Hertie-Institute for Clinical Brain Research, Tubingen, Germany

[14]Karolinska Institutet, Department NVS, Division of Neurogeriatrics, Stockholm, Sweden

[15]Unit for Hereditray Dementia, Theme Aging, Karolinska University Hospital-Solna Stockholm Sweden

[16]Campbell Cognitive Neurology Research Unit, Sunnybrook Research Institute, Toronto, ON, Canada

[17]Toronto Western Hospital, Tanz Centre for Research in Neurodegenerative Disease, Toronto, ON, Canada

[18]Department of Clinical Neurosciences and Cambridge University Hospitals NHS Trust and Medical Research Council Cognition and brain Sciences Unit, University of Cambridge, Cambridge, United Kingdom

[19]Laboratory for Cognitive Neurology, Department of Neurosciences, KU Leuven, Leuven, Belgium

[20]Department of Clinical Neurological Sciences, University of Western Ontario, London, ON, Canada

[21]Fondazione Istituto di Ricovero e Cura a Carattere Scientifico, Istituto Neurologico Carlo Besta, Milan, Italy

[22]Faculty of Medicine, University of Lisbon, Lisbon, Portugal

[23]Neurology Department, Centro Hospitalar e Universitário de Coimbra, Portugal

[24]Department of Clinical Neurology, University of Oxford, Oxford, United Kingdom

[25]Department of Neurology and Neurosurgery, McGill University, Montreal, Quebec, Canada

[26]Division of Neuroscience and Experimental Psychology, Wolfson Molecular Imaging Centre, University of Manchester, Manchester, United Kingdom

[27]Departments of Geriatric Medicine and Nuclear Medicine, University of Duisburg-Essen, Germany

[28]Neurologische Klinik und Poliklinik, Ludwig-Maximilians-Universität, Munich; German Center for Neurodegenerative Diseases (DZNE), Munich; Munich Cluster of Systems Neurology, Munich, Germany

[29]Department of Neurology, University Hospital Ulm, Ulm, Germany

[30]Department of Neuroscience, Psychology, Drug Research and Child Health, University of Florence, Florence, Italy

[31]Sorbonne Université, Paris Brain Institute – Institut du Cerveau– ICM, Inserm U1127, CNRS UMR 7225, AP-HP - Hôpital Pitié-Salpêtrière, Paris, France

[32]Centre deréférence des démences rares ou précoces, IM2A, Département de Neurologie, AP-HP - Hôpital Pitié-Salpêtrière, Paris, France

[33]Département de Neurologie, AP-HP - Hôpital Pitié-Salpêtrière, Paris, France

[34]Univ Lille, France

[35]Inserm 1172, Lille, France

[36]CHU, CNR-MAJ, Labex Distalz, LiCENDLille, France

*See Appendix for a list of GENFI consortium members.

Corresponding author

Dr Jonathan D. Rohrer, Dementia Research Centre, Department of Neurodegenerative Disease, UCL Queen Square Institute of Neurology, 8-11 Queen Square, London, WC1N 3BG, United Kingdom; j.rohrer@ucl.ac.uk

Keywords: genetic frontotemporal dementia, MRI imaging, brain volumetry, presymptomatic stage

Word Count: 3441; Figure: 3; Table: 1.

Abstract

Background: Studies have previously shown evidence for presymptomatic cortical atrophy in genetic FTD. Whilst initial investigations have also identified early deep grey matter volume loss, little is known about the extent of subcortical involvement, particularly within subregions, and how this differs between genetic groups.

Methods: 480 mutation carriers from the Genetic FTD Initiative (GENFI) were included (198 *GRN*, 202 *C9orf72*, 80 *MAPT*), together with 298 non-carrier cognitively normal controls. Cortical and subcortical volumes of interest were generated using automated parcellation methods on volumetric 3T T1-weighted MRI scans. Mutation carriers were divided into three disease stages based on their global CDR® plus NACC FTLD score: asymptomatic (0), possibly or mildly symptomatic (0.5) and fully symptomatic (1 or more).

Results: In all three groups, subcortical involvement was seen at the CDR 0.5 stage prior to phenoconversion, whereas in the *C9orf72* and *MAPT* mutation carriers there was also involvement at the CDR 0 stage. In the *C9orf72* expansion carriers the earliest volume changes were in thalamic subnuclei (particularly pulvinar and lateral geniculate, 9-10%) cerebellum (lobules VIIa-Crus II and VIIIb, 2-3%), hippocampus (particularly presubiculum and CA1, 2-3%), amygdala (all subregions, 2-6%) and hypothalamus (superior tuberal region, 1%). In *MAPT* mutation carriers changes were seen at CDR 0 in the hippocampus (subiculum, presubiculum and tail, 3-4%) and amygdala (accessory basal and superficial nuclei, 2-4%). *GRN* mutation carriers showed subcortical differences at CDR 0.5 in the presubiculum of the hippocampus (8%).

Conclusions: *C9orf72* expansion carriers show the earliest and most widespread changes including the thalamus, basal ganglia and medial temporal lobe. By investigating individual subregions, changes can also be seen at CDR 0 in *MAPT* mutation carriers within the limbic system. Our results suggest that subcortical brain volumes may be used as markers of neurodegeneration even prior to the onset of prodromal symptoms.

Introduction

Frontotemporal dementia (FTD) is a common cause of early onset dementia. In about a third of the cases it is associated with an autosomal dominant inherited mutation in one of three genes: microtubule-associated protein tau (*MAPT*), progranulin (*GRN*), and chromosome 9 open reading frame 72 (*C9orf72*).[1] For each of these genetic groups, there is evidence of a differential pattern of cortical atrophy[2], with changes occurring presymptomatically, up to twenty years before estimated phenoconversion[3-4]. Whilst these studies have been highly informative in describing the presence of brain changes in presymptomatic stages of the disease, they have focused less on subcortical structures, and in particular, they have not investigated specific subregions within the deep grey matter. However, due to advanced imaging methods, it is now possible to measure these individual nuclei and subregions *in vivo* on structural magnetic resonance scans, with prior studies in small cohorts showing changes at the symptomatic stage of genetic FTD[5-8], but without any previous investigation of the presymptomatic period. Using data from the Genetic FTD Initiative (GENFI) cohort, we therefore aimed to examine the specific pattern of subcortical changes (including specific subregions), to determine which areas were impaired across the different disease stages of genetic FTD.

Methods

At the time of the fifth data freeze in the GENFI 2 study (03/03/2015-31/05/2019), 850 participants had been recruited across 24 centres in the United Kingdom, Canada, Italy, the Netherlands, Sweden, Portugal, Germany, France, Spain, and Belgium, of whom 804 had a volumetric T1-weighted magnetic resonance image acquired on a 3T scanner. Another 26 participants were excluded as the scans were of unsuitable quality due to motion or other imaging artefacts, pathology unlikely to be attributed to

FTD, or as they were carriers of mutations in one of the rarer genetic causes of FTD. All the remaining 778 participants were known to be either a carrier of a pathogenic expansion in *C9orf72* or of a pathogenic mutation in *GRN* or *MAPT* (n=480), or were non-carrier first-degree relatives (n=298), who therefore acted as controls within the study. All aspects of the study were approved by the local ethics committee for each of the GENFI sites, and written informed consent was obtained from all participants.

All participants underwent a standardized clinical assessment as described previously[3]. This included the CDR® plus NACC FTLD[9] which was used to group the mutation carriers into stages: those with a global score of 0 were considered as asymptomatic, those with a score of 0.5 considered as possibly or mildly symptomatic (i.e. prodromal), and those with a score ≥1 were considered as fully symptomatic or phenoconverted (**Table 1**).

Participants underwent a 1.1-mm isotropic resolution volumetric T1-weighted magnetic resonance imaging (MRI) on a 3T scanner (Siemens Trio, Siemens Skyra, Siemens Prisma, Philips Achieva, GE Discovery MR750). Volumetric MRI scans were first bias field corrected and whole brain parcellated using the geodesic information flow (GIF) algorithm[10], which is based on atlas propagation and label fusion. We combined regions of interest to calculate grey matter volumes of the cortex for 15 regions: orbitofrontal, dorsolateral (DLPFC) and ventromedial prefrontal, motor, anterior and posterior insula, temporal pole, dorsolateral and medial temporal, anterior and posterior cingulate, sensory, medial and lateral parietal, and occipital cortex. Using GIF and customised versions of specific Freesurfer modules[11-14] that accept the GIF parcellation as inputs[6-8,15] we also calculated individual volumes for the following subcortical regions (**Figure 1**): i) basal ganglia (nucleus accumbens, caudate, putamen,

and globus pallidus, ii) basal forebrain, iii) amygdala (5 regions: lateral nucleus, basal and paralaminar nucleus, accessory basal nucleus, cortico-amygdaloid transition area and the superficial nuclei), iv) hippocampus (7 regions: cornu ammonis CA1, CA2/CA3, CA4, dentate gyrus, subiculum, presubiculum, tail), v) thalamus (14 regions: anteroventral, laterodorsal (LD), lateral posterior, ventral anterior, ventral lateral anterior, ventral lateral posterior, ventral posterolateral, ventromedial, intralaminar, midline, mediodorsal (MD), lateral geniculate (LGN), medial geniculate (MGN) and pulvinar). Volumes for the hypothalamus (5 regions: anterior superior, anterior inferior, superior tuberal (s-tub), inferior tuberal (i-tub), posterior) were computed using the deep convolutional neural network method described in [16]. We also parcellated the cerebellum (separated into 14 regions: lobules I-IV, V, VI, VIIa-Crus I, VIIa-Crus II, VIIb, VIIIa, VIIIb, IX, X, vermis, dentate nucleus, interposed nucleus and fastigial nucleus[17-18]), and brainstem (superior cerebellar peduncle, medulla, pons, and midbrain).

Left and right volumes were summed, and total intracranial volume was computed with SPM12 v6470 (Statistical Parametric Mapping, Wellcome Trust Centre for Neuroimaging, London, UK) running under Matlab R2014b (Math Works, Natick, MA, USA)[19]. All segmentations were visually checked for quality with only one subject excluded from the cerebellar analyses due to the presence of an arachnoid cyst. Statistical analyses were performed in SPSS software (SPSS Inc., Chicago, IL, USA) version 26, with a linear regression analysis within each genetic group adjusting for age, sex, and scanner type (as there were significant differences between groups for each of these, **Table 1**), as well as total intracranial volume, with correction for multiple comparisons using the Benjamini & Hochberg method[20] using p=0.05 for false discovery rate. The correction was performed separately for the genetic groups (*MAPT*, *GRN*, *C9orf72*), while considering the number of comparisons within each

of the main regions (cortical, cerebellum, brainstem, thalamus, hypothalamus, amygdala, hippocampus, and other subcortical structures).

Results

Total brain and cortical volumes

The total brain volume was significantly smaller in all genetic groups with CDR ≥1 when compared to controls (8-10% volumetric difference, $p<0.0005$). However, it was also significantly smaller in *C9orf72* expansion carriers at CDR 0 and 0.5 (1-3%, $p\leq0.004$) (**Supplementary Table 1**, **Supplementary Figure 1**).

C9orf72 expansion carriers with a CDR ≥1 showed significantly smaller volumes than controls in all cortical regions, with the largest differences in the anterior and posterior insula (24%) (**Supplementary Table 1, Supplementary Figure 2**). These two regions, together with the DLPFC, motor, dorsolateral temporal, lateral parietal and occipital cortex, were also significantly smaller in the *C9orf72* expansion carriers with CDR 0 and 0.5 (2-7%, $p\leq0.006$). The temporal pole was significantly smaller than controls in those scoring 0.5 (6%, $p=0.004$), while the orbitofrontal, posterior cingulate, sensory and medial parietal cortex were significantly smaller in those scoring 0 (1-4%, $p\leq0.028$), but these differences did not reach statistical significance in those scoring 0.5 (**Supplementary Table 1, Supplementary Figure 2**).

MAPT mutation carriers with CDR ≥1 showed smaller volumes than controls in the temporal regions (32% in the temporal pole), insula (29-30%) and anterior cingulate (12%) ($p<0.0005$) (**Supplementary**

Table 1, Supplementary Figure 2). The dorsolateral temporal cortex was smaller in the CDR 0.5 group (17%, p=0.003). No difference was found in the CDR 0 group.

GRN mutation carriers with CDR ≥1 showed smaller volumes in all regions (6-26%, p≤0.012) except the sensory cortex, with the anterior insula being the region with smallest volume (26%, p<0.0005). *GRN* mutation carriers with CDR 0.5 also showed smaller DLPFC and anterior insula volumes than controls (5-6%, p≤0.013) (**Supplementary Table 1, Supplementary Figure 2**). No difference was found in the CDR 0 group.

Basal ganglia

Among the basal ganglia, the putamen was significantly smaller across all *C9orf72* stages (1-17%, p≤0.0006) (**Supplementary Table 1, Figure 2A**), and in the *MAPT* and *GRN* mutation carriers with CDR ≥1 (17%, p<0.0005). *C9orf72* expansion carriers with CDR 0.5 and ≥1 showed smaller globus pallidus (6-16%, p≤0.003). *MAPT* mutation carriers with CDR ≥1 showed smaller volumes than controls in the nucleus accumbens (11%), and globus pallidus (14%), whilst *GRN* mutation carriers scoring ≥1 showed smaller caudate (5%, p=0.011) and globus pallidus (12%, p<0.0005). No differences were found for the *MAPT* and *GRN* mutation carriers in the CDR 0 or 0.5 groups.

Basal forebrain

Changes in the basal forebrain were only seen in *MAPT* mutation carriers (**Supplementary Table 1, Figure 2A**), and only at the CDR ≥1 stage (15% smaller than controls, p<0.0005).

Amygdala

All amygdalar regions were significantly smaller than controls for all mutation carriers with CDR ≥1 (p<0.0005), with the *MAPT* group showing the largest differences, particularly in the superficial and accessory basal regions (44%) as well as the lateral regions (36%) (**Supplementary Table 1, Figure 2B**). All regions were significantly smaller in *C9orf72* expansion carriers at CDR 0, and in *MAPT* mutation carriers with CDR 0.5, with smaller volumes at CDR 0 in the superficial and accessory basal nuclei (2-4%, p≤0.034) (**Supplementary Table 1, Figure 2B**). *GRN* mutation carriers with CDR 0 or 0.5 did not show any significant differences from controls.

Hippocampus

All hippocampal regions were significantly smaller than controls for all mutation carriers with CDR ≥1 (p<0.0005), with *MAPT* mutation carriers being the genetic group with the largest differences (all above 30%) (**Supplementary Table 1, Figure 2C**). Differences were also seen in all regions in *MAPT* mutation carriers with CDR 0.5 (6-11%, p≤0.019), and in the subiculum, presubiculum and tail (3-4%, p≤0.020) in *MAPT* mutation carriers with CDR 0. In *C9orf72* expansion carriers with CDR 0 there were significantly smaller volumes than controls in all regions except the tail and the subiculum (2-3%, p≤0.015). The presubiculum was the only region significantly smaller in *GRN* mutation carriers with CDR 0.5 (8%, p=0.016) with no significant differences at CDR 0.

Thalamus

C9orf72 expansion carriers showed significantly smaller thalamic regions in all stages, with the only exception being the ventromedial nucleus (which only became significant at CDR stage ≥1) and the ventral posterolateral nucleus, which did not quite reach statistical significance at CDR 0.5. The most affected regions at CDR 0 were the LD (13%), LGN (10%) and pulvinar (9%) (p<0.0005)

(**Supplementary Table 1, Figure 2D**). *MAPT* mutation carriers with CDR ≥1 showed significantly smaller volumes in all regions except LGN, with the main differences located in the MD, midline and LD regions (22-26%, p<0.0005) but no differences at earlier stages. *GRN* mutation carriers also only showed significantly smaller regions at CDR ≥1, with the main differences located in the MD and midline regions (31%, p<0.0005), followed by the anteroventral and LD (21- 25%, p<0.0005). No differences were found in the LGN and MGN.

Hypothalamus

All regions were significantly smaller than controls for all mutation carriers with CDR ≥1 (p<0.0005), except for the i-tub regions for *C9orf72* and *GRN* mutation carriers. In the CDR ≥1 group *MAPT* mutation carriers had the smallest volumes, with differences above 29% in the posterior and anterior regions (**Supplementary Table 1, Figure 2E**). *C9orf72* expansion carriers were the only ones showing early differences, with the CDR 0.5 group showing smaller volumes than controls in the anterior superior and s-tub regions (5-7%, p≤0.017), and the CDR 0 group showing smaller volumes than controls in the s-tub region (1%, p=0.008).

Cerebellum

C9orf72 and *GRN* mutation carriers with CDR ≥1 had smaller volumes than controls in the lobules VIIa-Crus II (13%), VIIb (11-12%) and VIIIa (8-10%) (p≤0.001), with *C9orf72* expansion carriers also showing significant differences in lobules VI (12%), VIIIb (14%), vermis (7%) and the dentate nucleus (7%) (p≤0.007). In addition, the *C9orf72* expansion carriers were the only group with significantly smaller volumes at CDR 0 (lobules VIIa-Crus II and VIIb, 2-3% p≤0.011) (**Supplementary Table 1**, **Figure 2F**). No significant difference was found in the *MAPT* group.

Brainstem

GRN mutation carriers with CDR ≥1 showed smaller volumes in the superior cerebellar peduncle (5%, p=0.011), midbrain and pons (7-8%, p<0.0005), while *MAPT* mutation carriers scoring ≥1 showed smaller volumes in the midbrain (9%, p<0.0005) (**Supplementary Table 1**, **Figure 2G**). No difference was detected in those with CDR 0 or 0.5, or in *C9orf72* expansion carriers at any stage.

Figure 3 summarizes the sequential pattern of neuroanatomical involvement for each of the genetic groups, by indicating at which stage each region resulted significantly smaller than controls.

Discussion

In this study we have defined the pattern of involvement in subcortical brain regions and specific nuclei in genetic frontotemporal dementia. We have identified gene-specific changes in asymptomatic and prodromal stages through to fully symptomatic stages in *C9orf72*, *MAPT* and *GRN* mutation carriers. By looking at specific regions, in a large cohort of mutation carriers, we were able to identify small changes that occurs very early on in all genetic groups, which might go undetected when looking at the whole brain or at large regions.

The first brain regions showing differences from controls in *C9orf72* expansion carriers without any detectable clinical symptoms were the thalamic regions (the pulvinar, LD and LGN in particular), the putamen, the CA regions with the dentate gyrus and the presubiculum, all the amygdalar regions, the s-tub region in the hypothalamus, the lobule VIIa-Crus II and VIIb of the cerebellum as well as several cortical regions. By the time *C9orf72* expansion carriers reach the symptomatic phase, nearly all the

regions in the brain become affected, with the exception of the caudate, nucleus accumbens, basal forebrain, brainstem, and the anterior and inferior cerebellum and the i-tub region of the hypothalamus. These results are in line with previous studies showing widespread involvement of the brain in *C9orf72*-associated FTD, well beyond the classical frontal and temporal regions of FTD.[3-4,21-22]

Among the thalamic regions, the pulvinar and LGN were particularly affected in *C9orf72* expansion carriers, which is in line with previous research in both symptomatic and presymptomatic carriers[8,22] and with the pathological accumulation of TDP-43 and dipeptide repeat proteins in those regions.[23-24] Atrophy in these regions is linked to hallucinations and other psychotic symptoms as well as the altered processing of pain, features seen more commonly in *C9orf72* expansion carriers than in other forms of FTD.[25-28]

Interestingly, the regions affected early in the cerebellum (lobule VIIa-Crus II and VIIb) are connected via the dentate nuclei to the ventral anterior and VL nuclei of the thalamus and from here to the DLPFC to regulate cognitive functions, and in particular goal-directed complex behaviours.[29-31] The cerebellum is also connected via the anterior and ventral lateral posterior thalamic regions to the basal ganglia and the parietal and motor cortex,[31-31] all regions affected early in *C9orf72*-associated FTD. Dipeptide repeat proteins are also typical and abundant in the cerebellar cortex.[32]

The most affected regions within the hippocampus and amygdala are among the ones previously shown to be atrophic in symptomatic *C9orf72* expansion carriers[6-7] and connected to the temporal and

posterior cortex.[33] The CA regions are abundant of dipeptide repeat proteins, with or without TDP-43 deposition.[34]

C9orf72 expansion carriers at CDR 0 showed reduced volumes in the s-tub region of the hypothalamus and later on in the anterior and posterior hypothalamus, leaving the i-tub as the only spared region as previously reported.[35] The s-tub region includes the dorso-medial nucleus and lateral hypothalamic area, which regulate appetite and contain neuropeptide-expressing neurons and neuropeptide receptors.[36] Similarly, volume loss in the posterior hypothalamus and the presence of TDP-43 pathology have been linked to the development of abnormal eating behaviours, typical symptoms of bvFTD. [35,37]

In *MAPT* mutation carriers, the only regions affected at CDR 0 were the superficial and accessory basal regions of the amygdala, and the subiculum, presubiculum and hippocampal tail. Such early differences in the amygdala could not be detected when looking at its volume as a whole, which only became significantly affected at a later stage. *MAPT* mutation carriers at CDR 0.5 additionally showed smaller volumes in the dorsolateral temporal cortex and in all the other hippocampal and amygdalar regions. Overall, the more medial regions of the amygdala (particularly the superficial, accessory basal and basal and paralaminar) tend to be affected more than the lateral regions. They are connected to key limbic regions and likely related to the development of symptoms associated with abnormal reward and emotional processing. These results are in line with previous *in vivo* studies on symptomatic mutation carriers[6-7] and with pathological studies: tau deposition is extensively found in the hippocampus and other limbic structures in *MAPT* mutation carriers.[38]

By the time *MAPT* mutation carriers are fully symptomatic, we find lower volumes in the other key regions of the limbic system, such as the insula, anterior cingulate, mediotemporal cortex, nucleus accumbens and basal forebrain. This latter structure, the basal forebrain, was only affected in the *MAPT* genetic group, as previously reported.[39] Other regions affected in this group include the midbrain, which forms part of a network that regulates emotion perception with the thalamus and amygdala.[40] All regions in the hypothalamus were also affected, although mainly in the superior and posterior regions as previously reported in a smaller cohort.[35] Interestingly, the posterior region includes the mammillary bodies, connected via the fornix to the amygdala and hippocampus. Among the thalamic regions, the MD was the most affected, as previously reported[8]: this region is connected to brain regions within the limbic network and plays a role in emotional and behavioural regulation, as well as executive function. This sequence of regional involvement and the localisation in the temporal lobe is in line with what has been reported in other studies in *MAPT* mutation carriers.[3-4,41-42] The vermis of the cerebellum, another important part of the limbic system, was not affected, in contrast with what was found by another study.[5] This could be due to the different way of classifying the symptomatic mutation carriers, and the presence of different scanner types and sample characteristics. However, the fact that the cerebellum was overall not affected in *MAPT*-associated FTD is in line with other studies.[3]

GRN mutation carriers only showed significant atrophy at the CDR 0.5 stage – this was mainly cortical, affecting the DLPFC, and anterior insula, but there was also subcortical involvement of the presubiculum, a hippocampal region connected to the basal ganglia, frontal and parietal cortex, areas which are typically atrophic in *GRN*, as found here at the symptomatic stages and in other studies,[3-4,42] and which typically show TDP-43 accumulation.[34]

Previously described as spared in *GRN* mutation carriers,[5] we found here that lobule VIIa-Crus II, VIIb and VIIIa are affected later in the disease. These regions are connected, via the thalamus, to the DLPFC and primary sensorimotor cortex.[29] Within the brainstem, the midbrain, pons, and superior cerebellar peduncle were atrophic, as previously found.[43] The role of the brainstem in FTD is not yet fully understood, but TDP-43 pathology has been found previously in several nuclei of the midbrain and pons.[44] When symptoms were clearly present in *GRN* mutation carriers, all the hypothalamic regions were also smaller than in controls, with the exception of the i-tub (similarly to the *C9orf72* group). This region includes the arcuate nucleus, an important target for metabolic and hormonal signals.[36] Interestingly, in a previous histological study (and consistent with our findings), TDP-43 inclusions were not found in this region, but were abundant in the anterior, superior and posterior region of the hypothalamus.[45]

C9orf72 expansion carriers showed by far the earliest and most widespread changes in the brain, compared to *MAPT* and *GRN* mutation carriers. Even the total brain volume was lower in *C9orf72* expansion carriers at CDR 0 whilst only being affected at the fully symptomatic stage in *MAPT* and *GRN* mutation carriers. This result was found previously[3] and could suggest that *C9orf72*-associated FTD might be associated with a long and slow process of neurodegeneration which could start many decades before the onset of clinical symptoms, as also suggested by Staffaroni *et al*[46]. *GRN* mutation carriers instead might have a more rapid process which occurs later and closer to symptom onset.[47] Longitudinal studies, such as in Staffaroni *et al*[46] and Whitwell *et al*[48], looking at the atrophy rates in the different disease stages could potentially provide a definite answer to whether this is the case.

This study has some limitations. Some of the nuclei are very small and we grouped them into combined regions, or clusters of nuclei. In the future, this could be addressed by imaging at higher field strengths (e.g. 7T), enabling higher spatial resolution. There were differences in age, sex and scanner type for some of the groups, which we have taken into account by including these variables as covariates, although this cannot completely exclude their impact. The CDR 0.5 is smaller than the other groups, and is likely to be heterogeneous including both people who are truly in a mild prodromal stage, and others that score 0.5 due to 'questionable' symptoms that might instead be related to affective symptoms during the at-risk period.

By looking at *in vivo* regional volumetry, we have shown here a differential pattern of subcortical changes across severity stages in *GRN*, *MAPT* and *C9orf72* mutation carriers. By looking at a wide range of specific brain regions, for the first time we were able to measure small changes that occur in localized regions in the early stages of genetic FTD. These results suggest that these changes may be used as markers of neurodegeneration in future trials even during preclinical and prodromal periods. Further longitudinal studies, including multimodal imaging looking at brain connectivity networks and including correlations with cognitive and other biomarkers, will be vital to investigate these results further.

Acknowledgments

We thank the research participants for their contribution to the study. The Dementia Research Centre is supported by Alzheimer's Research UK, Alzheimer's Society, Brain Research UK, and The Wolfson Foundation. This work was supported by the National Institute for Health Research (NIHR) Queen Square Dementia Biomedical Research Unit and the University College London Hospitals Biomedical Research Centre, the Leonard Wolfson Experimental Neurology Centre (LWENC) Clinical Research Facility, and the UK Dementia Research Institute, which receives its funding from UK DRI Ltd, funded by the UK Medical Research Council, Alzheimer's Society and Alzheimer's Research UK. This work was also supported by the MRC UK GENFI grant (MR/M023664/1), the Italian Ministry of Health (CoEN015 and Ricerca Corrente), the Canadian Institutes of Health Research as part of a Centres of Excellence in Neurodegeneration grant, a Canadian Institutes of Health Research operating grant, the Alzheimer's Society grant (AS-PG-16-007), the Bluefield Project and the JPND GENFI-PROX grant (2019-02248). MB is supported by a Fellowship award from the Alzheimer's Society, UK (AS-JF-19a-004-517). MB's work was also supported by the UK Dementia Research Institute which receives its funding from DRI Ltd, funded by the UK Medical Research Council, Alzheimer's Society and Alzheimer's Research UK. MB acknowledges the support of NVIDIA Corporation with the donation of the Titan V GPU used for part of the analyses in this research. JDR is an MRC Clinician Scientist (MR/M008525/1) and has received funding from the NIHR Rare Diseases Translational Research Collaboration (BRC149/NS/MH), the Bluefield Project and the Association for Frontotemporal Degeneration. JEI is supported by the European Research Council (Starting Grant 677697, project BUNGEE-TOOLS), Alzheimer's Research UK (ARUK-IRG2019A003) and NIH 1RF1MH123195-01. JBR is funded by the Wellcome Trust (103838) and the National Institute for Health Research Cambridge Biomedical Research Centre. This work was funded by the Deutsche

Forschungsgemeinschaft (DFG, German Research Foundation) under Germany's Excellence Strategy within the framework of the Munich Cluster for Systems Neurology (EXC 2145 SyNergy – ID 390857198). Several authors of this publication (JCvS, MS, RSV, AD, MO, JDR) are members of the European Reference Network for Rare Neurological Diseases (ERN-RND) - Project ID No 739510.

Appendix. GENFI Consortium Authors

- Sónia Afonso - Instituto Ciencias Nucleares Aplicadas a Saude, Universidade de Coimbra, Coimbra, Portugal;
- Maria Rosario Almeida - Faculty of Medicine, University of Coimbra, Coimbra, Portugal;
- Sarah Anderl-Straub – Department of Neurology, University of Ulm, Ulm, Germany;
- Christin Andersson - Department of Clinical Neuroscience, Karolinska Institutet, Stockholm, Sweden;
- Anna Antonell - Alzheimer's disease and Other Cognitive Disorders Unit, Neurology Service, Hospital Clínic, Barcelona, Spain;
- Silvana Archetti - Biotechnology Laboratory, Department of Diagnostics, ASST Brescia Hospital, Brescia, Italy;
- Andrea Arighi - Fondazione IRCCS Ca' Granda Ospedale Maggiore Policlinico, Neurodegenerative Diseases Unit, Milan, Italy; University of Milan, Centro Dino Ferrari, Milan, Italy;
- Mircea Balasa - Alzheimer's disease and Other Cognitive Disorders Unit, Neurology Service, Hospital Clínic, Barcelona, Spain;
- Myriam Barandiaran - Cognitive Disorders Unit, Department of Neurology, Donostia University Hospital, San Sebastian, Gipuzkoa, Spain; Neuroscience Area, Biodonostia Health Research Insitute, San Sebastian, Gipuzkoa, Spain;
- Nuria Bargalló - Imaging Diagnostic Center, Hospital Clínic, Barcelona, Spain;
- Robart Bartha - Department of Medical Biophysics, The University of Western Ontario, London, Ontario, Canada; Centre for Functional and Metabolic Mapping, Robarts Research Institute, The University of Western Ontario, London, Ontario, Canada;
- Benjamin Bender - Department of Diagnostic and Interventional Neuroradiology, University of Tübingen, Tübingen, Germany;
- Alberto Benussi - Centre for Neurodegenerative Disorders, Department of Clinical and Experimental Sciences, University of Brescia, Italy;
- Maxime Bertoux – Inserm 1172, Lille, France; CHU, CNR-MAJ, Labex Distalz, LiCEND Lille, France;
- Anne Bertrand - Sorbonne Université, Paris Brain Institute – Institut du Cerveau – ICM, Inserm U1127, CNRS UMR 7225, AP-HP - Hôpital Pitié-Salpêtrière, Paris, France; Inria, Aramis project-team, F-75013, Paris, France; Centre pour l'Acquisition et le Traitement des Images, Institut du Cerveau et la Moelle, Paris, France
- Valentina Bessi - Department of Neuroscience, Psychology, Drug Research, and Child Health, University of Florence, Florence, Italy;
- Sandra Black - Sunnybrook Health Sciences Centre, Sunnybrook Research Institute, University of Toronto, Toronto, Canada;
- Sergi Borrego-Ecija - Alzheimer's disease and Other Cognitive Disorders Unit, Neurology Service, Hospital Clínic, Barcelona, Spain;
- Jose Bras - Center for Neurodegenerative Science, Van Andel Institute, Grand Rapids, Michigan, MI 49503, USA;
- Alexis Brice - Sorbonne Université, Paris Brain Institute – Institut du Cerveau – ICM, Inserm U1127, CNRS UMR 7225, AP-HP - Hôpital Pitié-Salpêtrière, Paris, France; Reference Network for Rare Neurological Diseases (ERN-RND);
- Rose Bruffaerts - Laboratory for Cognitive Neurology, Department of Neurosciences, KU Leuven, Leuven, Belgium;
- Agnès Camuzat - Sorbonne Université, Paris Brain Institute – Institut du Cerveau – ICM, Inserm U1127, CNRS UMR 7225, AP-HP - Hôpital Pitié-Salpêtrière, Paris, France;
- Marta Cañada - CITA Alzheimer, San Sebastian, Gipuzkoa, Spain
- Valentina Cantoni - Centre for Neurodegenerative Disorders, Neurology Unit, Department of Clinical and Experimental Sciences, University of Brescia, Brescia, Italy;
- Paola Caroppo - Fondazione IRCCS Istituto Neurologico Carlo Besta, Milano, Italy;
- Miguel Castelo-Branco - Faculty of Medicine, University of Coimbra, Coimbra, Portugal;

- Olivier Colliot - Sorbonne Université, Paris Brain Institute – Institut du Cerveau – ICM, Inserm U1127, CNRS UMR 7225, AP-HP - Hôpital Pitié-Salpêtrière, Paris, France; Inria, Aramis project-team, F-75013, Paris, France; Centre pour l'Acquisition et le Traitement des Images, Institut du Cerveau et la Moelle, Paris, France;
- Thomas Cope – Department of Clinical Neuroscience, University of Cambridge, Cambridge, UK;
- Vincent Deramecourt - Univ Lille, France; Inserm 1172, Lille, France; CHU, CNR-MAJ, Labex Distalz, LiCEND Lille, France;
- María de Arriba - Neuroscience Area, Biodonostia Health Research Insitute, San Sebastian, Gipuzkoa, Spain;
- Giuseppe Di Fede - Fondazione IRCCS Istituto Neurologico Carlo Besta, Milano, Italy;
- Alina Díez - Neuroscience Area, Biodonostia Health Research Insitute, San Sebastian, Gipuzkoa, Spain
- Diana Duro - Faculty of Medicine, University of Coimbra, Coimbra, Portugal;
- Chiara Fenoglio - Fondazione IRCCS Ca' Granda Ospedale Maggiore Policlinico, Neurodegenerative Diseases Unit, Milan, Italy; University of Milan, Centro Dino Ferrari, Milan, Italy;
- Camilla Ferrari - Department of Neuroscience, Psychology, Drug Research, and Child Health, University of Florence, Florence, Italy;
- Catarina B. Ferreira -Laboratory of Neurosciences, Institute of Molecular Medicine, Faculty of Medicine, University of Lisbon, Lisbon, Portugal;
- Nick Fox – Dementia Research Centre, Department of Neurodegenerative Disease, UCL Institute of Neurology, Queen Square, London, UK;
- Morris Freedman - Baycrest Health Sciences, Rotman Research Institute, University of Toronto, Toronto, Canada;
- Giorgio Fumagalli - Fondazione IRCCS Ca' Granda Ospedale Maggiore Policlinico, Neurodegenerative Diseases Unit, Milan, Italy; University of Milan, Centro Dino Ferrari, Milan, Italy;
- Aurélie Funkiewiez - Centre de référence des démences rares ou précoces, IM2A, Département de Neurologie, AP-HP - Hôpital Pitié-Salpêtrière, Paris, France; Sorbonne Université, Paris Brain Institute – Institut du Cerveau – ICM, Inserm U1127, CNRS UMR 7225, AP-HP - Hôpital Pitié-Salpêtrière, Paris, France;
- Alazne Gabilondo -Neuroscience Area, Biodonostia Health Research Insitute, San Sebastian, Gipuzkoa, Spain;
- Roberto Gasparotti - Neuroradiology Unit, University of Brescia, Brescia, Italy
- Serge Gauthier - Alzheimer Disease Research Unit, McGill Centre for Studies in Aging, Department of Neurology & Neurosurgery, McGill University, Montreal, Québec, Canada;
- Stefano Gazzina - Neurology, ASST Brescia Hospital, Brescia, Italy
- Giorgio Giaccone - Fondazione IRCCS Istituto Neurologico Carlo Besta, Milano, Italy;
- Ana Gorostidi - Neuroscience Area, Biodonostia Health Research Insitute, San Sebastian, Gipuzkoa, Spain;
- Caroline Greaves – Dementia Research Centre, Department of Neurodegenerative Disease, UCL Institute of Neurology, Queen Square, London, UK;
- Rita Guerreiro - Center for Neurodegenerative Science, Van Andel Institute, Grand Rapids, Michigan, MI 49503, USA;
- Carolin Heller – Dementia Research Centre, Department of Neurodegenerative Disease, UCL Institute of Neurology, Queen Square, London, UK;
- Tobias Hoegen - Neurologische Klinik, Ludwig-Maximilians-Universität München, Munich, Germany;
- Begoña Indakoetxea - Cognitive Disorders Unit, Department of Neurology, Donostia University Hospital, San Sebastian, Gipuzkoa, Spain; Neuroscience Area, Biodonostia Health Research Insitute, San Sebastian, Gipuzkoa, Spain;
- Vesna Jelic - Division of Clinical Geriatrics, Karolinska Institutet, Stockholm, Sweden;
- Hans-Otto Karnath - Division of Neuropsychology, Hertie-Institute for Clinical Brain Research and Center of Neurology, University of Tübingen, Tübingen, Germany;
- Ron Keren -The University Health Network, Toronto Rehabilitation Institute, Toronto, Canada;

- Gregory Kuchcinski - Univ Lille, France; Inserm 1172, Lille, France; CHU, CNR-MAJ, Labex Distalz, LiCEND Lille, France;
- Tobias Langheinrich - Division of Neuroscience and Experimental Psychology, Wolfson Molecular Imaging Centre, University of Manchester, Manchester, UK; Manchester Centre for Clinical Neurosciences, Department of Neurology, Salford Royal NHS Foundation Trust, Manchester, UK;
- Thibaud Lebouvier - Univ Lille, France; Inserm 1172, Lille, France; CHU, CNR-MAJ, Labex Distalz, LiCEND Lille, France;
- Maria João Leitão - Centre of Neurosciences and Cell Biology, Universidade de Coimbra, Coimbra, Portugal;
- Albert Lladó - Alzheimer's disease and Other Cognitive Disorders Unit, Neurology Service, Hospital Clínic, Barcelona, Spain;
- Gemma Lombardi - Department of Neuroscience, Psychology, Drug Research and Child Health, University of Florence, Florence, Italy;
- Sandra Loosli -Neurologische Klinik, Ludwig-Maximilians-Universität München, Munich, Germany;
- Carolina Maruta - Laboratory of Language Research, Centro de Estudos Egas Moniz, Faculty of Medicine, University of Lisbon, Lisbon, Portugal;
- Simon Mead - MRC Prion Unit, Department of Neurodegenerative Disease, UCL Institute of Neurology, Queen Square, London, UK;
- Lieke Meeter - Department of Neurology, Erasmus Medical Center, Rotterdam, Netherlands;
- Gabriel Miltenberger - Faculty of Medicine, University of Lisbon, Lisbon, Portugal;
- Rick van Minkelen - Department of Clinical Genetics, Erasmus Medical Center, Rotterdam, Netherlands;
- Sara Mitchell - Sunnybrook Health Sciences Centre, Sunnybrook Research Institute, University of Toronto, Toronto, Canada;
- Katrina Moore – Dementia Research Centre, Department of Neurodegenerative Disease, UCL Institute of Neurology, Queen Square, London UK;
- Benedetta Nacmias - Department of Neuroscience, Psychology, Drug Research and Child Health, University of Florence, Florence, Italy;
- Annabel Nelson - Dementia Research Centre, Department of Neurodegenerative Disease, UCL Institute of Neurology, Queen Square, London, UK;
- Jennifer Nicholas - Department of Medical Statistics, London School of Hygiene and Tropical Medicine, London, UK;
- Linn Öijerstedt - Center for Alzheimer Research, Division of Neurogeriatrics, Department of Neurobiology, Care Sciences and Society, Bioclinicum, Karolinska Institutet, Solna, Sweden; Unit for Hereditary Dementias, Theme Aging, Karolinska University Hospital, Solna, Sweden;
- Jaume Olives - Alzheimer's disease and Other Cognitive Disorders Unit, Neurology Service, Hospital Clínic, Barcelona, Spain;
- Sebastien Ourselin - School of Biomedical Engineering & Imaging Sciences, King's College London, London, UK;
- Alessandro Padovani - Centre for Neurodegenerative Disorders, Department of Clinical and Experimental Sciences, University of Brescia, Italy
- Jessica Panman – Department of Neurology, Erasmus Medical Center, Rotterdam, Netherlands;
- Janne M. Papma - Department of Neurology, Erasmus Medical Center, Rotterdam;
- Yolande Pijnenburg - Amsterdam University Medical Centre, Amsterdam VUmc, Amsterdam, Netherlands;
- Cristina Polito - Department of Biomedical, Experimental and Clinical Sciences "Mario Serio", Nuclear Medicine Unit, University of Florence, Florence, Italy
- Enrico Premi - Stroke Unit, ASST Brescia Hospital, Brescia, Italy
- Sara Prioni - Fondazione IRCCS Istituto Neurologico Carlo Besta, Milano, Italy;
- Catharina Prix -Neurologische Klinik, Ludwig-Maximilians-Universität München, Munich, Germany;

- Rosa Rademakers [as London Ontario geneticist] - Department of Neurosciences, Mayo Clinic, Jacksonville, Florida, USA;
- Veronica Redaelli -Fondazione IRCCS Istituto Neurologico Carlo Besta, Milano, Italy;
- Daisy Rinaldi - Centre de référence des démences rares ou précoces, IM2A, Département de Neurologie, AP-HP - Hôpital Pitié-Salpêtrière, Paris, France; Sorbonne Université, Paris Brain Institute – Institut du Cerveau – ICM, Inserm U1127, CNRS UMR 7225, AP-HP - Hôpital Pitié-Salpêtrière, Paris, France; Département de Neurologie, AP-HP - Hôpital Pitié-Salpêtrière, Paris, France; Reference Network for Rare Neurological Diseases (ERN-RND);
- Tim Rittman – Department of Clinical Neurosciences, University of Cambridge, Cambridge, UK;
- Ekaterina Rogaeva -Tanz Centre for Research in Neurodegenerative Diseases, University of Toronto, Toronto, Canada;
- Adeline Rollin - CHU, CNR-MAJ, Labex Distalz, LiCEND Lille, France;
- Pedro Rosa-Neto -Translational Neuroimaging Laboratory, McGill Centre for Studies in Aging, McGill University, Montreal, Québec, Canada;
- Giacomina Rossi - Fondazione IRCCS Istituto Neurologico Carlo Besta, Milano, Italy;
- Martin Rossor – Dementia Research Centre, Department of Neurodegenerative Disease, UCL Institute of Neurology, Queen Square, London, UK;
- Beatriz Santiago - Neurology Department, Centro Hospitalar e Universitario de Coimbra, Coimbra, Portugal;
- Dario Saracino – Sorbonne Université, Paris Brain Institute – Institut du Cerveau – ICM, Inserm U1127, CNRS UMR 7225, AP-HP - Hôpital Pitié-Salpêtrière, Paris, France; Inria, Aramis project-team, F-75013, Paris, France; Centre de référence des démences rares ou précoces, IM2A, Département de Neurologie, AP-HP - Hôpital Pitié-Salpêtrière, Paris, France;
- Sabrina Sayah - Sorbonne Université, Paris Brain Institute – Institut du Cerveau – ICM, Inserm U1127, CNRS UMR 7225, AP-HP - Hôpital Pitié-Salpêtrière, Paris, France;
- Elio Scarpini - Fondazione IRCCS Ca' Granda Ospedale Maggiore Policlinico, Neurodegenerative Diseases Unit, Milan, Italy; University of Milan, Centro Dino Ferrari, Milan, Italy;
- Sonja Schönecker - Neurologische Klinik, Ludwig-Maximilians-Universität München, Munich, Germany;
- Elisa Semler -Department of Neurology, University of Ulm, Ulm;
- Rachelle Shafei – Dementia Research Centre, Department of Neurodegenerative Disease, UCL Institute of Neurology, Queen Square, London, UK;
- Christen Shoesmith - Department of Clinical Neurological Sciences, University of Western Ontario, London, Ontario, Canada;
- Imogen Swift - Department of Neurodegenerative Disease, Dementia Research Centre, UCL Institute of Neurology, Queen Square, London, UK;
- Miguel Tábuas-Pereira - Neurology Department, Centro Hospitalar e Universitario de Coimbra, Coimbra, Portugal;
- Mikel Tainta - Neuroscience Area, Biodonostia Health Research Insitute, San Sebastian, Gipuzkoa, Spain;
- Ricardo Taipa - Neuropathology Unit and Department of Neurology, Centro Hospitalar do Porto - Hospital de Santo António, Oporto, Portugal;
- David Tang-Wai -The University Health Network, Krembil Research Institute, Toronto, Canada;
- Paul Thompson - Division of Neuroscience and Experimental Psychology, Wolfson Molecular Imaging Centre, University of Manchester, Manchester, UK;
- Hakan Thonberg - Center for Alzheimer Research, Division of Neurogeriatrics, Karolinska Institutet, Stockholm, Sweden;
- Carolyn Timberlake – Department of Clinical Neurosciences, University of Cambridge, Cambridge, UK;
- Pietro Tiraboschi - Fondazione IRCCS Istituto Neurologico Carlo Besta, Milano, Italy;
- Philip Van Damme - Neurology Service, University Hospitals Leuven, Belgium; Laboratory for Neurobiology, VIB-KU Leuven Centre for Brain Research, Leuven, Belgium;

- Mathieu Vandenbulcke - Geriatric Psychiatry Service, University Hospitals Leuven, Belgium; Neuropsychiatry, Department of Neurosciences, KU Leuven, Leuven, Belgium;
- Michele Veldsman - Nuffield Department of Clinical Neurosciences, Medical Sciences Division, University of Oxford, Oxford, UK;
- Ana Verdelho - Department of Neurosciences and Mental Health, Centro Hospitalar Lisboa Norte - Hospital de Santa Maria & Faculty of Medicine, University of Lisbon, Lisbon, Portugal;
- Jorge Villanua - OSATEK, University of Donostia, San Sebastian, Gipuzkoa, Spain;
- Jason Warren – Dementia Research Centre, Department of Neurodegenerative Disease, UCL Institute of Neurology, Queen Square, London, UK;
- Carlo Wilke - Department of Neurodegenerative Diseases, Hertie-Institute for Clinical Brain Research and Center of Neurology, University of Tübingen, Tübingen, Germany; Center for Neurodegenerative Diseases (DZNE), Tübingen, Germany;
- Ione Woollacott – Dementia Research Centre, Department of Neurodegenerative Disease, UCL Institute of Neurology, Queen Square, London, UK;
- Elisabeth Wlasich - Neurologische Klinik, Ludwig-Maximilians-Universität München, Munich, Germany;
- Henrik Zetterberg - Dementia Research Institute, Department of Neurodegenerative Disease, UCL Institute of Neurology, Queen Square, London, UK;
- Miren Zulaica - Neuroscience Area, Biodonostia Health Research Insitute, San Sebastian, Gipuzkoa, Spain.

References

1. Warren JD, Rohrer JD, Rossor MN. Clinical review. Frontotemporal dementia. BMJ 2013;347:f4827.
2. Chen Q, Kantarci K. Imaging Biomarkers for Neurodegeneration in Presymptomatic Familial Frontotemporal Lobar Degeneration. Front Neurol. 2020;11:80.
3. Rohrer JD, Nicholas JM, Cash DM, et al. Presymptomatic cognitive and neuroanatomical changes in genetic frontotemporal dementia in the Genetic Frontotemporal dementia Initiative (GENFI) study: a cross-sectional analysis. Lancet Neurol. 2015;14(3):253-62.
4. Cash DM, Bocchetta M, Thomas D, et al. Patterns of grey matter atrophy in genetic frontotemporal dementia: results from the GENFI study. Neurobiology of Aging 2018; 62:191-196.
5. Bocchetta M, Cardoso MJ, Cash DM, Ourselin S, Warren JD, Rohrer JD. Patterns of regional cerebellar atrophy in genetic frontotemporal dementia. Neuroimage Clin. 2016; 11: 287–290.
6. Bocchetta M, Iglesias JE, Scelsi MA, et al. Hippocampal subfield volumetry: differential pattern of atrophy in different forms of genetic frontotemporal dementia. Journal of Alzheimer's Disease 2018;64(2):497-504.
7. Bocchetta M, Iglesias JE, Cash DM, Warren JD, Rohrer JD. Amygdala subnuclei are differentially affected in the different genetic and pathological forms of frontotemporal dementia. Alzheimer's & Dementia: Diagnosis, Assessment & Disease Monitoring. 2019;11:136-141.

8. Bocchetta M, Iglesias JE, Neason M, Cash DM, Warren JD, Rohrer JD. Thalamic nuclei in frontotemporal dementia: mediodorsal nucleus involvement is universal but pulvinar atrophy is unique to C9orf72. Human Brain Mapping 2020;41(4):1006-1016.
9. Miyagawa T, Brushaber D, Syrjanen J, et al. Utility of the global CDR® plus NACC FTLD rating and development of scoring rules: Data from the ARTFL/LEFFTDS Consortium. Alzheimer's & dementia: the journal of the Alzheimer's Association. 2020;16(1):106–117.
10. Cardoso MJ, Modat M, Wolz R, et al. Geodesic information flows: spatially-variant graphs and their application to segmentation and fusion. IEEE TMI 2015 doi: 10.1109/TMI.2015.2418298.
11. Iglesias JE, Augustinack JC, Nguyen K, et al. A computational atlas of the hippocampal formation using ex vivo, ultra-high resolution MRI: Application to adaptive segmentation of in vivo MRI. Neuroimage. 2015. 115:117-137.
12. Iglesias JE, Van Leemput K, Bhatt P, et al. Bayesian segmentation of brainstem structures in MRI. Neuroimage. 2015;113:184-95.
13. Iglesias JE, Insausti R, Lerma-Usabiaga G, et al. A probabilistic atlas of the human thalamic nuclei combining ex vivo MRI and histology. Neuroimage. 2018.183:314-326.
14. Saygin ZM, Kliemann D, Iglesias JE, et al. High-resolution magnetic resonance imaging reveals nuclei of the human amygdala: manual segmentation to automatic atlas. Neuroimage. 2017;155:370-382.
15. Bocchetta M, Iglesias JE, Chelban V, et al. Automated brainstem segmentation detects differential involvement in atypical parkinsonian syndromes. Journal of Movement Disorders. 2020;13(1):39-46.

16. Billot B, Bocchetta M, Todd E, Dalca A, Rohrer J, Iglesias Gonzalez JE. Automated segmentation of the Hypothalamus and associated subunits in brain MRI. Neuroimage. 2020:117287, doi: 10.1016/j.neuroimage.2020.117287.
17. Diedrichsen J, Balsters JH, Flavell J, Cussans E, Ramnani N. A probabilistic MR atlas of the human cerebellum. NeuroImage. 2009;46(1):39-46.
18. Diedrichsen J, Maderwald S, Küper M, et al. Imaging the deep cerebellar nuclei: a probabilistic atlas and normalization procedure. NeuroImage 2011;54(3):1786-1794.
19. Malone IB, Leung KK, Clegg S, et al. Accurate automatic estimation of total intracranial volume: a nuisance variable with less nuisance. Neuroimage. 2015;104:366-72.
20. Benjamini Y and Hochberg Y. Controlling the False Discovery Rate: A Practical and Powerful Approach to Multiple Testing. Journal of the Royal Statistical Society: Series B (Methodological). 1995; 57(1):289-300.
21. Bertrand A, Wen J, Rinaldi D, et al. Early Cognitive, Structural, and Microstructural Changes in Presymptomatic C9orf72 Carriers Younger Than 40 Years. JAMA Neurol. 2018;75(2):236-245..
22. Lee SE, Sias AC, Mandelli ML, et al. Network degeneration and dysfunction in presymptomatic C9ORF72 expansion carriers. Neuroimage Clin. 2016;14:286-297.
23. Vatsavayai SC, Yoon SJ, Gardner RC, et al. Timing and significance of pathological features in C9orf72 expansion-associated frontotemporal dementia. Brain. 2016;139(Pt 12):3202-3216.
24. Yang Y, Halliday GM, Hodges JR, Tan RH. von Economo Neuron Density and Thalamus Volumes in Behavioral Deficits in Frontotemporal Dementia Cases with and without a C9ORF72 Repeat Expansion. J Alzheimers Dis. 2017;58(3):701-709.

25. Convery RS, Bocchetta M, Greaves CV, et al. Abnormal pain perception is associated with thalamo-cortico-striatal atrophy in C9orf72 expansion carriers in the GENFI cohort. J Neurol Neurosurg Psychiatry. 2020:jnnp-2020-323279. doi: 10.1136/jnnp-2020-323279.
26. Ducharme S, Bajestan S, Dickerson BC, Voon V. Psychiatric presentations of C9orf72 mutation: What are the diagnostic implica- tions for clinicians? Journal of Neuropsychiatry and Clinical Neurosciences. 2017;29(3),195–205.
27. Fletcher PD, Downey LE, Golden HL, et al. Pain and temperature processing in dementia: A clinical and neuroanatomical analysis. Brain 2015; 138(Pt 11):3360–3372.
28. Kertesz A, Ang LC, Jesso S, et al. Psychosis and hallucinations in frontotemporal dementia with the C9ORF72 mutation: a detailed clinical cohort. Cogn Behav Neurol. 2013;26(3):146-54.
29. Makris N, Hodge SM, Haselgrove C, et al. Human cerebellum: surface-assisted cortical parcellation and volumetry with magnetic resonance imaging. J Cogn Neurosci. 2003;15(4):584-99.
30. D'Angelo E, Casali S. Seeking a unified framework for cerebellar function and dysfunction: from circuit operations to cognition. Front Neural Circuits. 2013 10;6:116.
31. Palesi F, Tournier JD, Calamante F, et al. Contralateral cerebello-thalamo-cortical pathways with prominent involvement of associative areas in humans in vivo. Brain Struct Funct. 2015;220(6):3369-84.
32. Mackenzie IR, Neumann M. Molecular neuropathology of frontotemporal dementia: insights into disease mechanisms from postmortem studies. J Neurochem. 2016;138 Suppl 1:54-70.

33. de Flores R, Mutlu J, Bejanin A, et al. Intrinsic connectivity of hippocampal subfields in normal elderly and mild cognitive impairment patients. Hum Brain Mapp. 2017;38(10):4922-4932.

34. Mann DMA, Snowden JS. Frontotemporal lobar degeneration: Pathogenesis, pathology and pathways to phenotype. Brain Pathol. 2017;27(6):723-736.

35. Bocchetta M, Gordon E, Manning E, et al. Detailed volumetric analysis of the hypothalamus in behavioral variant frontotemporal dementia. Journal of Neurology 2015;262(12):2635-2642.

36. Parker JA, Bloom SR. Hypothalamic neuropeptides and the regulation of appetite. Neuropharmacology. 2012;63(1):18-30.

37. Piguet O, Petersen A, Yin Ka Lam B, et al. Eating and hypothalamus changes in behavioral-variant frontotemporal dementia. Ann Neurol. 2011;69:312–319.

38. Ghetti B, Oblak AL, Boeve BF, Johnson KA, Dickerson BC, Goedert M. Invited review: Frontotemporal dementia caused by microtubule-associated protein tau gene (MAPT) mutations: a chameleon for neuropathology and neuroimaging. Neuropathol Appl Neurobiol. 2015;41(1):24-46.

39. Convery RS, Neason MR, Cash DM, et al. Basal forebrain atrophy in frontotemporal dementia. NeuroImage: Clinical. 2020;26:102210.

40. Liddell BJ, Brown KJ, Kemp AH, et al. A direct brainstem-amygdala-cortical 'alarm' system for subliminal signals of fear. Neuroimage. 2005;24(1):235-43.

41. Whitwell JL, Weigand SD, Boeve BF, et al. Neuroimaging signatures of frontotemporal dementia genetics: C9ORF72, tau, progranulin and sporadics. Brain. 2012;135(Pt 3):794-806.

42. Olney NT, Ong E, Goh SM, et al. Clinical and volumetric changes with increasing functional impairment in familial frontotemporal lobar degeneration. Alzheimers Dement. 2020;16(1):49-59.

43. Rohrer JD, Ridgway GR, Modat M, et al. Distinct profiles of brain atrophy in frontotemporal lobar degeneration caused by progranulin and tau mutations. Neuroimage. 2010;53(3):1070-6.

44. Grinberg LT, Rueb U, Heinsen H. Brainstem: neglected locus in neurodegenerative diseases. Front Neurol. 2011;11;2:42.

45. Cykowski MD, Takei H, Van Eldik LJ, et al. Hippocampal Sclerosis but Not Normal Aging or Alzheimer Disease Is Associated With TDP-43 Pathology in the Basal Forebrain of Aged Persons. J Neuropathol Exp Neurol. 2016;75(5):397-407.

46. Staffaroni AM, Goh SM, Cobigo Y, et al. Rates of Brain Atrophy Across Disease Stages in Familial Frontotemporal Dementia Associated With MAPT, GRN, and C9orf72 Pathogenic Variants. JAMA Netw Open. 2020;3(10):e2022847.

47. Jiskoot LC, Panman JL, Meeter LH, et al. Longitudinal multimodal MRI as prognostic and diagnostic biomarker in presymptomatic familial frontotemporal dementia. Brain. 2019;142(1):193-208.

48. Whitwell JL, Boeve BF, Weigand SD, et al. Brain atrophy over time in genetic and sporadic frontotemporal dementia: a study of 198 serial magnetic resonance images. Eur J Neurol. 2015;22(5):745-52.

Table 1: Demographic and clinical characteristic of the cohort divided by genetic group and CDR®+NACC FTLD global scores. Abbreviations: N/A not applicable, FTD frontotemporal dementia, bvFTD behavioural variant FTD, PPA primary progressive aphasia, NOS not otherwise specified, CBS corticobasal syndrome, PSP progressive supranuclear palsy, AD Alzheimer's disease, ALS amyotrophic lateral sclerosis.

	Non-carriers	*C9orf72* mutation carriers			*MAPT* mutation carriers			*GRN* mutation carriers		
CDR®+NACC FTLD global score		**0**	**0.5**	**≥1**	**0**	**0.5**	**≥1**	**0**	**0.5**	**≥1**
N	298	107	32	63	47	13	20	125	30	43
Age, year	45.8 (12.5)	43.9 (11.7)	49.4 (11.7)	62.9 (9.2)	39.3 (10.6)	47.0 (12.0)	58.2 (10.1)	45.5 (12.0)	52.0 (13.3)	63.6 (8.2)
Sex, male (%)	125 (41.9%)	44 (41.1%)	12 (37.5%)	41 (65.1%)	20 (42.6%)	4 (30.8%)	13 (65.0%)	43 (34.4%)	15 (50%)	21 (48.8%)
Scanners [Siemens Trio/Siemens Skyra/Siemens Prisma/Philips Achieva/GE Discovery MR750]	59/64/79/94/2	32/14/19/42/0	4/4/10/14/0	8/11/27/16/1	11/11/8/16/1	1/1/8/3/0	6/2/10/2/0	39/20/16/45/5	5/7/9/8/1	11/11/14/7/0
Clinical phenotype	N/A	N/A	N/A	49 bvFTD, 6 FTD-ALS, 2 ALS, 2 PPA, 1 PSP, 2 Dementia-NOS, 1 Other	N/A	N/A	16 bvFTD, 1 PPA, 2 Dementia-NOS, 1 PSP	N/A	N/A	24 bvFTD, 17 PPA, 1 CBS, 1 AD

Figure 1. **Regions of interest used in the analysis.** Abbreviations. Cortical: VMPFC ventromedial prefrontal, TP temporal pole, MT medial temporal, AC anterior cingulate, PC posterior cingulate, MOT motor, S sensory, MP medial parietal, OCC occipital, DLPFC dorsolateral prefrontal, OF orbitofrontal, AI anterior insular, PI posterior insular, DLT dorsolateral temporal, LP lateral parietal; Basal ganglia and Basal forebrain: GP pallidum, CAU caudate, PUT putamen, BF basal forebrain, NA nucleus accumbens; Brainstem: SCP superior cerebellar peduncle, MB midbrain, ME medulla; Cerebellum: VIIA – CI lobule VIIA – Crus I, VIIA – CII lobule VIIA – Crus II, FN fastigial nucleus, IN interposed nucleus, DN dentate nucleus; Amygdala: CAT cortico-amygdaloid transition area, Sup superficial nuclei, AB accessory basal nucleus; Hippocampus: DG dentate gyrus, CA cornu ammonis; Thalamus: AV anteroventral, VA ventral anterior, LD laterodorsal, VLa ventral lateral anterior, MD mediodorsal, LP lateral posterior, VLp ventral lateral posterior, VPL ventral posterolateral, VM ventromedial, LGN lateral geniculate nucleus, MGN medial geniculate nucleus; Hypothalamus: as anterior superior, ai anterior inferior, s-tub superior tuberal, i-tub inferior tuberal, pos posterior.

Cortex

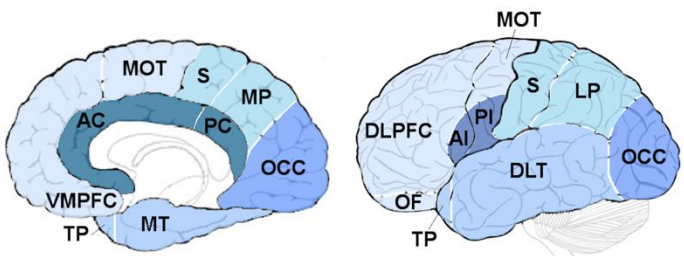

Basal ganglia and Basal forebrain

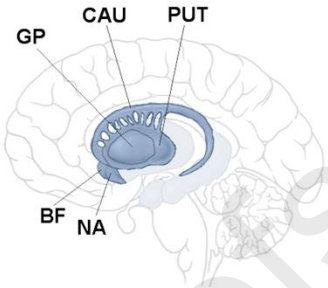

Brainstem and Cerebellum

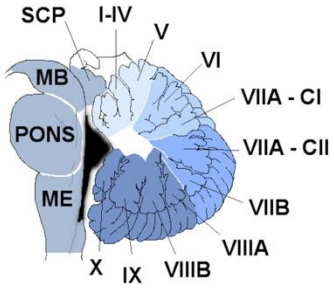

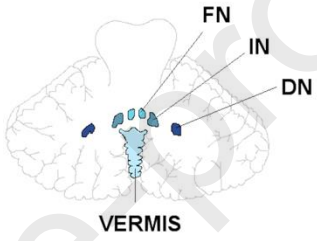

Amygdala

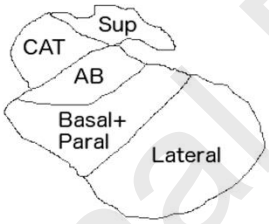

Hippocampus

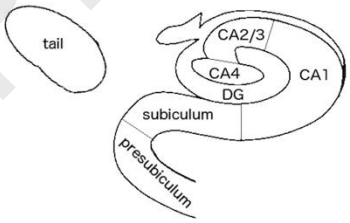

Thalamus

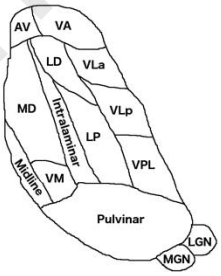

Hypothalamus

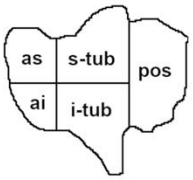

Figure 2A-G. Plots representing the means and standard error bars for regional brain volumes for each of the stages in *C9orf72*, *MAPT* and *GRN* mutation carriers. Volumes as expressed as % the mean volumes in controls (y axis). * indicates a significant difference from controls after correcting for multiple comparisons. Abbreviations: CAT cortico-amygdaloid transition area; Thalamus: LD laterodorsal, VLa ventral lateral anterior, VLp ventral lateral posterior, VPL ventral posterolateral, LGN lateral geniculate nucleus, MGN medial geniculate nucleus; Hypothalamus: AI anterior inferior, AS anterior superior, I-TUB inferior tuberal, S-TUB superior tuberal; Brainstem: SCP superior cerebellar peduncle.

Figure 3. Sequential pattern of neuroanatomical involvement in *C9orf72*, *MAPT* and *GRN*. The colour map indicates the stage defined by CDR®+NACC FTLD global scores when the specific region of interest becomes involved, as significantly smaller than controls.

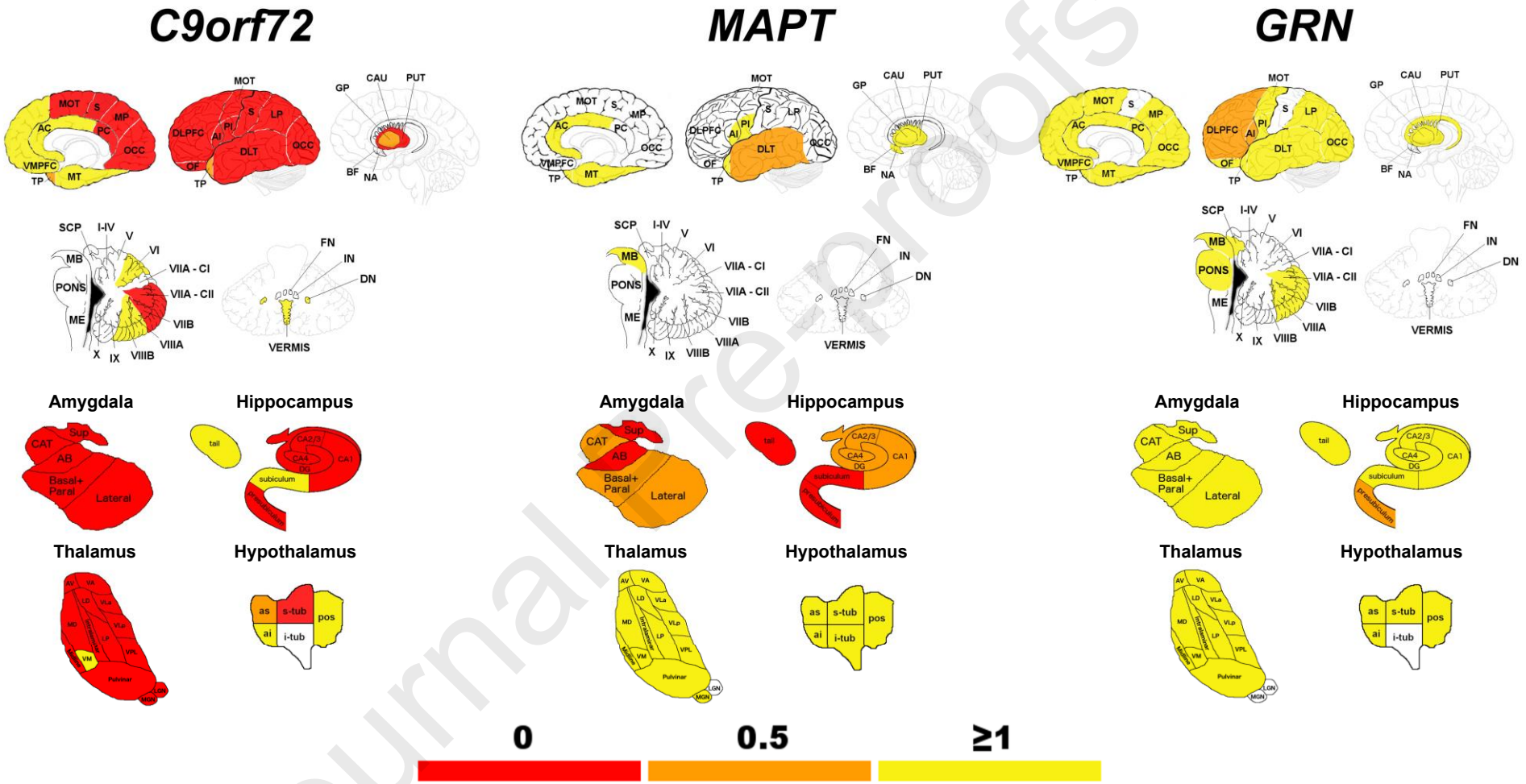

Supplementary material

Supplementary Table 1: Volumetric comparisons for the brain regions between the different subgroups and the controls. Volumetric comparisons, expressed as % of total intracranial volume, are adjusted for age, sex, total intracranial volume, and scanner type. Bold and italics represents a significant difference between groups after correcting for multiple comparisons. The % difference represents the volumetric difference between each group and controls. Abbreviations: Cortical: OF orbitofrontal, DLPFC dorsolateral prefrontal, VMPFC ventromedial prefrontal, Mot motor, AI anterior insular, PI posterior insular, TP temporal pole, DLT dorsolateral temporal, MT medial temporal, AC anterior cingulate, PC posterior cingulate, S sensory, MP medial parietal, LP lateral parietal, Occ occipital; Cerebellum: DN dentate nucleus, IN interposed nucleus, FN fastigial nucleus; Basal ganglia and Basal forebrain: NA nucleus accumbens, Cau caudate, Put putamen, GP pallidum, BF basal forebrain; Thalamus: AV anteroventral, LD laterodorsal, LP lateral posterior, VA ventral anterior, VLa ventral lateral anterior, VLp ventral lateral posterior, VPL ventral posterolateral, VM ventromedial, Int intralaminar, Mid midline, MD mediodorsal, LGN lateral geniculate nucleus, MGN medial geniculate nucleus, Pul Pulvinar; Amygdala: Sup superficial nuclei, CAT cortico-amygdaloid transition area, AB accessory basal nucleus; BL basal and paralaminar nuclei, LN lateral nucleus; Hippocampus: CA cornu ammonis, DG dentate gyrus, Sub Subiculum, Pre presubiculum; Brainstem: SCP superior cerebellar peduncle, MB midbrain, ME medulla; Hypothalamus: as anterior superior, ai anterior inferior, s-tub superior tuberal, i-tub inferior tuberal, pos posterior.

Groups		Brain	OF	DLPFC	VMPFC	Mot	AI	PI	TP	DLT	MT	AC	PC	S	MP	LP	Occ
			Cortical														
non-carriers	Mean	80.20	1.45	6.27	1.97	2.82	0.50	0.25	0.98	5.53	2.00	1.32	0.68	1.41	1.39	3.77	5.15
	SD	3.22	0.10	0.43	0.16	0.21	0.04	0.02	0.10	0.33	0.13	0.11	0.06	0.14	0.14	0.28	0.43
C9orf72		Brain	OF	DLPFC	VMPFC	Mot	AI	PI	TP	DLT	MT	AC	PC	S	MP	LP	Occ
CDR®+NACC-FTLD global score = 0	Mean	79.17	1.44	6.15	1.97	2.77	0.49	0.25	0.97	5.41	2.00	1.31	0.67	1.37	1.34	3.66	5.00
	SD	3.02	0.11	0.50	0.18	0.21	0.05	0.02	0.09	0.35	0.12	0.11	0.06	0.12	0.12	0.30	0.40
CDR®+NACC-FTLD global score = 0.5	Mean	78.04	1.42	6.01	1.93	2.68	0.47	0.24	0.92	5.27	1.96	1.30	0.66	1.35	1.33	3.60	4.88
	SD	3.35	0.12	0.49	0.20	0.27	0.06	0.03	0.10	0.32	0.11	0.12	0.06	0.14	0.16	0.32	0.45
CDR®+NACC-FTLD global score ≥ 1	Mean	72.30	1.26	5.24	1.71	2.43	0.38	0.19	0.86	4.78	1.85	1.18	0.61	1.21	1.22	3.21	4.56
	SD	4.43	0.12	0.63	0.19	0.30	0.06	0.03	0.13	0.40	0.16	0.10	0.07	0.14	0.15	0.30	0.45
% difference	CDR®+NACC-FTLD global score = 0	1.3	1.0	1.9	-0.2	1.9	1.9	3.4	1.6	2.2	0.2	1.0	2.0	2.2	3.5	2.9	3.0
	CDR®+NACC-FTLD global score = 0.5	2.7	2.1	4.1	1.8	5.0	6.1	7.2	6.1	4.8	2.1	2.2	2.4	3.7	4.8	4.6	5.3
	CDR®+NACC-FTLD global score ≥ 1	9.8	12.9	16.5	13.1	14.0	24.1	23.7	12.0	13.6	7.4	10.7	9.8	14.0	12.1	14.9	11.5
p-value	CDR®+NACC-FTLD global score = 0	***<0.0005***	***0.028***	***0.004***	0.496	***0.004***	***0.003***	***<0.0005***	0.079	***<0.0005***	0.242	0.109	***0.010***	***0.003***	***<0.0005***	***<0.0005***	***<0.0005***
	CDR®+NACC-FTLD global score = 0.5	***0.004***	0.206	***0.006***	0.859	***0.004***	***0.001***	***<0.0005***	***0.004***	***<0.0005***	0.255	0.234	0.307	0.069	0.057	***0.003***	***0.005***
	CDR®+NACC-FTLD global score ≥ 1	***<0.0005***	***<0.0005***	***<0.0005***	***<0.0005***	***<0.0005***	***<0.0005***	***<0.0005***	***<0.0005***	***<0.0005***	***<0.0005***	***<0.0005***	***0.001***	***<0.0005***	***<0.0005***	***<0.0005***	***<0.0005***
MAPT		Brain	OF	DLPFC	VMPFC	Mot	AI	PI	TP	DLT	MT	AC	PC	S	MP	LP	Occ
CDR®+NACC-FTLD global score = 0	Mean	80.72	1.46	6.28	1.95	2.79	0.51	0.26	0.98	5.55	2.02	1.33	0.72	1.41	1.39	3.79	5.10
	SD	2.51	0.10	0.36	0.18	0.19	0.06	0.02	0.12	0.40	0.15	0.11	0.06	0.12	0.13	0.30	0.42
CDR®+NACC-FTLD global score = 0.5	Mean	79.34	1.43	6.14	1.99	2.81	0.48	0.24	0.91	5.28	1.94	1.29	0.66	1.38	1.35	3.69	5.12
	SD	2.62	0.09	0.36	0.18	0.18	0.07	0.03	0.14	0.39	0.16	0.08	0.03	0.14	0.12	0.22	0.55
CDR®+NACC-FTLD global score ≥ 1	Mean	74.07	1.36	5.84	1.86	2.71	0.36	0.18	0.67	4.58	1.70	1.16	0.65	1.37	1.35	3.49	4.91
	SD	4.23	0.10	0.51	0.20	0.23	0.08	0.04	0.16	0.69	0.25	0.12	0.04	0.16	0.12	0.27	0.35
% difference	CDR®+NACC-FTLD global score = 0	-0.6	-0.9	-0.2	0.9	1.2	-1.3	-2.6	-0.3	-0.4	-1.0	-0.5	-5.2	0.0	0.3	-0.3	1.0
	CDR®+NACC-FTLD global score = 0.5	1.1	1.2	2.0	-0.9	0.4	5.0	3.7	6.9	4.5	3.2	2.7	3.6	1.6	2.7	2.2	0.6
	CDR®+NACC-FTLD global score ≥ 1	7.6	6.3	6.9	5.3	4.1	28.7	29.6	31.6	17.1	15.1	12.1	4.9	2.5	3.2	7.4	4.6
p-value	CDR®+NACC-FTLD global score = 0	0.667	0.929	0.392	0.077	0.048	0.737	0.954	0.939	0.127	0.821	0.639	***0.008***	0.584	0.230	0.177	0.055
	CDR®+NACC-FTLD global score = 0.5	0.102	0.296	0.124	0.675	0.650	0.021	0.034	0.029	***0.003***	0.028	0.172	0.242	0.391	0.456	0.136	0.899
	CDR®+NACC-FTLD global score ≥ 1	***<0.0005***	0.058	0.032	0.248	0.404	***<0.0005***	***<0.0005***	***<0.0005***	***<0.0005***	***<0.0005***	***<0.0005***	0.611	0.665	0.967	0.036	0.226
GRN		Brain	OF	DLPFC	VMPFC	Mot	AI	PI	TP	DLT	MT	AC	PC	S	MP	LP	Occ
CDR®+NACC-FTLD global score = 0	Mean	80.03	1.46	6.33	2.00	2.86	0.50	0.26	0.96	5.53	1.98	1.35	0.69	1.43	1.39	3.78	5.14
	SD	3.23	0.09	0.43	0.17	0.22	0.05	0.03	0.09	0.33	0.13	0.12	0.07	0.13	0.15	0.34	0.44
CDR®+NACC-FTLD global score = 0.5	Mean	78.19	1.41	5.96	1.89	2.72	0.47	0.25	0.96	5.33	1.96	1.28	0.68	1.36	1.35	3.67	4.93
	SD	4.57	0.13	0.57	0.18	0.25	0.06	0.03	0.09	0.41	0.15	0.14	0.08	0.15	0.15	0.34	0.38
CDR®+NACC-FTLD global score ≥ 1	Mean	71.90	1.27	5.04	1.73	2.37	0.37	0.21	0.90	4.73	1.88	1.13	0.60	1.33	1.20	3.24	4.80
	SD	4.99	0.16	0.73	0.25	0.30	0.07	0.03	0.12	0.50	0.16	0.13	0.08	0.16	0.18	0.38	0.50
% difference	CDR®+NACC-FTLD global score = 0	0.2	-0.9	-1.0	-1.4	-1.2	0.4	-0.7	1.7	0.0	1.0	-1.7	-1.0	-1.9	0.2	-0.3	0.2
	CDR®+NACC-FTLD global score = 0.5	2.5	2.8	4.9	4.1	3.5	6.4	1.8	2.7	3.6	1.9	3.1	-0.1	3.5	2.9	2.7	4.2
	CDR®+NACC-FTLD global score ≥ 1	10.4	12.3	19.5	11.9	15.9	25.9	19.0	8.6	14.6	6.1	14.6	11.5	5.6	13.5	14.0	6.9
p-value	CDR®+NACC-FTLD global score = 0	0.306	0.423	0.333	0.254	0.206	0.493	0.648	0.132	0.705	0.068	0.095	0.344	0.173	0.690	0.781	0.569
	CDR®+NACC-FTLD global score = 0.5	0.131	0.336	***0.013***	0.109	0.168	***0.012***	0.364	0.258	0.127	0.788	0.364	0.302	0.361	0.805	0.854	0.083
	CDR®+NACC-FTLD global score ≥ 1	***<0.0005***	***<0.0005***	***<0.0005***	***<0.0005***	***<0.0005***	***<0.0005***	***<0.0005***	***<0.0005***	***<0.0005***	***0.001***	***<0.0005***	***<0.0005***	0.261	***<0.0005***	***<0.0005***	***0.012***

Groups		NA	Cau	Put	GP	BF	Whole	Sup	CAT	AB	BL	LN
		Basal ganglia and Basal forebrain					Amygdala					
non-carriers	Mean	0.08	0.45	0.63	0.28	0.07	0.25	0.03	0.02	0.04	0.07	0.10
	SD	0.01	0.05	0.05	0.03	0.01	0.02	0.00	0.00	0.00	0.01	0.01
C9orf72		NA	Cau	Put	GP	BF	Whole	Sup	CAT	AB	BL	LN
CDR®+NACC-FTLD global score = 0	Mean	0.08	0.45	0.62	0.28	0.07	0.25	0.02	0.02	0.04	0.07	0.09
	SD	0.01	0.05	0.06	0.03	0.01	0.02	0.00	0.00	0.00	0.01	0.01
CDR®+NACC-FTLD global score = 0.5	Mean	0.07	0.44	0.59	0.26	0.07	0.24	0.02	0.02	0.04	0.07	0.09
	SD	0.01	0.06	0.07	0.03	0.01	0.03	0.00	0.00	0.00	0.01	0.01
CDR®+NACC-FTLD global score ≥ 1	Mean	0.07	0.43	0.52	0.23	0.07	0.20	0.02	0.02	0.03	0.06	0.08
	SD	0.01	0.07	0.07	0.03	0.01	0.04	0.00	0.00	0.01	0.01	0.01
% difference	CDR®+NACC-FTLD global score = 0	0.3	1.1	1.1	0.3	1.4	2.9	2.4	5.8	4.5	2.3	2.2
	CDR®+NACC-FTLD global score = 0.5	2.6	2.7	5.6	5.5	1.9	5.2	7.2	8.6	7.6	4.5	3.3
	CDR®+NACC-FTLD global score ≥ 1	5.1	5.9	16.9	16.3	6.0	19.6	24.0	27.6	25.4	20.3	13.9
p-value	CDR®+NACC-FTLD global score = 0	0.496	0.183	***0.006***	0.209	0.083	***<0.0005***	***0.002***	***<0.0005***	***<0.0005***	***0.001***	***0.006***
	CDR®+NACC-FTLD global score = 0.5	0.344	0.573	***0.001***	***0.003***	0.841	***0.004***	***0.002***	***<0.0005***	***<0.0005***	***0.033***	0.072
	CDR®+NACC-FTLD global score ≥ 1	0.058	0.053	***<0.0005***	***<0.0005***	0.477	***<0.0005***	***<0.0005***	***<0.0005***	***<0.0005***	***<0.0005***	***<0.0005***
MAPT		NA	Cau	Put	GP	BF	Whole	Sup	CAT	AB	BL	LN
CDR®+NACC-FTLD global score = 0	Mean	0.08	0.46	0.64	0.28	0.08	0.25	0.02	0.02	0.04	0.07	0.10
	SD	0.01	0.04	0.05	0.03	0.01	0.03	0.00	0.00	0.01	0.01	0.01
CDR®+NACC-FTLD global score = 0.5	Mean	0.08	0.46	0.65	0.28	0.07	0.23	0.02	0.02	0.03	0.06	0.09
	SD	0.01	0.05	0.07	0.03	0.01	0.04	0.00	0.00	0.01	0.01	0.02
CDR®+NACC-FTLD global score ≥ 1	Mean	0.07	0.44	0.52	0.24	0.06	0.15	0.01	0.01	0.02	0.04	0.06
	SD	0.01	0.06	0.07	0.02	0.01	0.05	0.00	0.00	0.01	0.01	0.02
% difference	CDR®+NACC-FTLD global score = 0	0.1	-2.4	-2.3	-2.3	-3.5	1.7	2.4	0.8	3.7	1.7	1.0
	CDR®+NACC-FTLD global score = 0.5	1.2	-2.5	-3.3	-2.8	6.5	11.0	9.6	12.8	13.4	11.4	9.9
	CDR®+NACC-FTLD global score ≥ 1	10.5	3.7	16.7	14.1	15.3	39.6	44.4	39.9	44.2	40.8	35.7
p-value	CDR®+NACC-FTLD global score = 0	0.628	0.204	0.392	0.350	0.243	0.064	***0.034***	0.063	***0.003***	0.058	0.418
	CDR®+NACC-FTLD global score = 0.5	0.632	0.503	0.601	0.954	0.031	***<0.0005***	***0.001***	***<0.0005***	***<0.0005***	***<0.0005***	***<0.0005***
	CDR®+NACC-FTLD global score ≥ 1	***<0.0005***	0.242	***<0.0005***	***<0.0005***	***<0.0005***	***<0.0005***	***<0.0005***	***<0.0005***	***<0.0005***	***<0.0005***	***<0.0005***
GRN		NA	Cau	Put	GP	BF	Whole	Sup	CAT	AB	BL	LN
CDR®+NACC-FTLD global score = 0	Mean	0.08	0.46	0.63	0.29	0.07	0.26	0.03	0.02	0.04	0.07	0.10
	SD	0.01	0.04	0.05	0.03	0.01	0.02	0.00	0.00	0.00	0.01	0.01
CDR®+NACC-FTLD global score = 0.5	Mean	0.07	0.46	0.61	0.27	0.07	0.25	0.02	0.02	0.04	0.07	0.10
	SD	0.01	0.06	0.06	0.03	0.01	0.03	0.00	0.00	0.00	0.01	0.01
CDR®+NACC-FTLD global score ≥ 1	Mean	0.07	0.43	0.52	0.24	0.07	0.22	0.02	0.02	0.03	0.06	0.09
	SD	0.01	0.07	0.06	0.02	0.01	0.03	0.00	0.00	0.01	0.01	0.01
% difference	CDR®+NACC-FTLD global score = 0	-0.7	-1.1	-0.9	-3.1	-0.7	-0.2	-2.8	1.6	-0.8	0.0	0.3
	CDR®+NACC-FTLD global score = 0.5	2.1	-1.1	3.5	1.1	5.0	1.8	4.4	4.5	3.9	1.7	-0.1
	CDR®+NACC-FTLD global score ≥ 1	3.7	5.3	17.2	12.0	6.2	14.3	20.4	21.4	18.8	14.6	9.1
p-value	CDR®+NACC-FTLD global score = 0	0.469	0.501	0.448	***0.005***	0.688	0.855	0.047	0.095	0.661	0.693	0.592
	CDR®+NACC-FTLD global score = 0.5	0.467	0.319	0.281	0.764	0.195	0.805	0.599	0.731	0.469	0.698	0.349
	CDR®+NACC-FTLD global score ≥ 1	0.233	***0.011***	***<0.0005***	***<0.0005***	0.364	***<0.0005***	***<0.0005***	***<0.0005***	***<0.0005***	***<0.0005***	***<0.0005***

Groups		Whole	CA1	CA2/3	CA4	DG	Sub	Pres	Tail
		Hippocampus							
non-carriers	Mean	0.50	0.09	0.03	0.04	0.04	0.06	0.05	0.09
	SD	0.04	0.01	0.00	0.00	0.00	0.01	0.01	0.01
C9orf72		Whole	CA1	CA2/3	CA4	DG	Sub	Pres	Tail
CDR®+NACC-FTLD global score = 0	Mean	0.49	0.09	0.03	0.04	0.04	0.06	0.05	0.08
	SD	0.04	0.01	0.00	0.00	0.00	0.01	0.01	0.01
CDR®+NACC-FTLD global score = 0.5	Mean	0.48	0.09	0.03	0.03	0.04	0.06	0.04	0.08
	SD	0.06	0.01	0.01	0.00	0.01	0.01	0.01	0.01
CDR®+NACC-FTLD global score ≥ 1	Mean	0.40	0.07	0.02	0.03	0.03	0.05	0.04	0.07
	SD	0.07	0.01	0.00	0.00	0.01	0.01	0.01	0.01
% difference	CDR®+NACC-FTLD global score = 0	2.0	2.8	1.9	1.7	2.2	0.7	1.7	1.3
	CDR®+NACC-FTLD global score = 0.5	3.8	5.0	1.9	2.0	2.9	3.6	5.7	1.2
	CDR®+NACC-FTLD global score ≥ 1	21.1	21.2	20.7	19.1	21.6	19.4	24.2	18.1
p-value	CDR®+NACC-FTLD global score = 0	***<0.0005***	***<0.0005***	***0.013***	***0.004***	***0.001***	0.110	***0.015***	0.043
	CDR®+NACC-FTLD global score = 0.5	***0.022***	***0.007***	0.171	0.134	0.058	0.080	***0.034***	0.573
	CDR®+NACC-FTLD global score ≥ 1	***<0.0005***	***<0.0005***	***<0.0005***	***<0.0005***	***<0.0005***	***<0.0005***	***<0.0005***	***<0.0005***
MAPT		Whole	CA1	CA2/3	CA4	DG	Sub	Pres	Tail
CDR®+NACC-FTLD global score = 0	Mean	0.49	0.09	0.03	0.04	0.04	0.06	0.05	0.08
	SD	0.06	0.01	0.00	0.00	0.00	0.01	0.01	0.01
CDR®+NACC-FTLD global score = 0.5	Mean	0.46	0.08	0.03	0.03	0.04	0.06	0.04	0.08
	SD	0.09	0.02	0.01	0.01	0.01	0.01	0.01	0.01
CDR®+NACC-FTLD global score ≥ 1	Mean	0.33	0.06	0.02	0.02	0.03	0.04	0.03	0.06
	SD	0.09	0.02	0.01	0.01	0.01	0.01	0.01	0.01
% difference	CDR®+NACC-FTLD global score = 0	1.9	1.7	1.0	0.0	-0.5	3.0	3.4	3.5
	CDR®+NACC-FTLD global score = 0.5	8.6	11.2	8.6	5.6	7.2	7.5	10.1	5.5
	CDR®+NACC-FTLD global score ≥ 1	35.0	35.6	36.6	32.6	34.4	33.1	37.6	30.8
p-value	CDR®+NACC-FTLD global score = 0	***0.025***	0.070	0.316	0.525	0.695	***0.020***	***0.006***	***0.014***
	CDR®+NACC-FTLD global score = 0.5	***<0.0005***	***<0.0005***	***0.003***	***0.006***	***0.002***	***0.003***	***<0.0005***	***0.019***
	CDR®+NACC-FTLD global score ≥ 1	***<0.0005***	***<0.0005***	***<0.0005***	***<0.0005***	***<0.0005***	***<0.0005***	***<0.0005***	***<0.0005***
GRN		Whole	CA1	CA2/3	CA4	DG	Sub	Pres	Tail
CDR®+NACC-FTLD global score = 0	Mean	0.51	0.09	0.03	0.04	0.04	0.06	0.05	0.09
	SD	0.05	0.01	0.00	0.00	0.00	0.01	0.01	0.01
CDR®+NACC-FTLD global score = 0.5	Mean	0.49	0.09	0.03	0.03	0.04	0.06	0.04	0.08
	SD	0.06	0.01	0.00	0.00	0.00	0.01	0.01	0.01
CDR®+NACC-FTLD global score ≥ 1	Mean	0.41	0.08	0.03	0.03	0.03	0.05	0.03	0.07
	SD	0.06	0.01	0.00	0.00	0.01	0.01	0.01	0.01
% difference	CDR®+NACC-FTLD global score = 0	-0.9	-0.8	-1.6	-2.0	-1.4	-1.0	0.6	-2.3
	CDR®+NACC-FTLD global score = 0.5	3.6	3.2	0.6	2.0	2.9	3.1	8.4	4.0
	CDR®+NACC-FTLD global score ≥ 1	18.6	16.6	15.0	13.5	16.6	18.0	27.7	16.7
p-value	CDR®+NACC-FTLD global score = 0	0.703	0.718	0.385	0.170	0.306	0.672	0.204	0.192
	CDR®+NACC-FTLD global score = 0.5	0.502	0.555	0.535	0.928	0.793	0.749	***0.016***	0.547
	CDR®+NACC-FTLD global score ≥ 1	***<0.0005***	***<0.0005***	***<0.0005***	***<0.0005***	***<0.0005***	***<0.0005***	***<0.0005***	***<0.0005***

Groups		Whole	AV	LD	LP	VA	VLa	VLp	VPL	VM	Int	Mid	MD	LGN	MGN	Pul
		Thalamus														
non-carriers	Mean	0.81	0.02	0.00	0.01	0.06	0.08	0.10	0.11	0.00	0.05	0.00	0.13	0.02	0.02	0.21
	SD	0.08	0.00	0.00	0.00	0.01	0.01	0.01	0.01	0.00	0.00	0.00	0.02	0.00	0.00	0.02
C9orf72		Whole	AV	LD	LP	VA	VLa	VLp	VPL	VM	Int	Mid	MD	LGN	MGN	Pul
CDR®+NACC-FTLD global score = 0	Mean	0.76	0.02	0.00	0.01	0.05	0.08	0.10	0.10	0.00	0.05	0.00	0.12	0.02	0.01	0.19
	SD	0.08	0.00	0.00	0.00	0.01	0.01	0.01	0.01	0.00	0.01	0.00	0.02	0.00	0.00	0.02
CDR®+NACC-FTLD global score = 0.5	Mean	0.74	0.01	0.00	0.01	0.05	0.07	0.10	0.10	0.00	0.05	0.00	0.11	0.02	0.01	0.18
	SD	0.08	0.00	0.00	0.00	0.01	0.01	0.01	0.01	0.00	0.01	0.00	0.02	0.00	0.00	0.02
CDR®+NACC-FTLD global score ≥ 1	Mean	0.67	0.01	0.00	0.01	0.05	0.07	0.09	0.10	0.00	0.04	0.00	0.09	0.02	0.01	0.16
	SD	0.08	0.00	0.00	0.00	0.01	0.01	0.01	0.01	0.00	0.01	0.00	0.02	0.00	0.00	0.02
% difference	CDR®+NACC-FTLD global score = 0	6.4	7.6	12.5	6.8	5.6	4.5	3.7	1.9	0.0	3.8	8.7	8.4	10.0	5.9	9.2
	CDR®+NACC-FTLD global score = 0.5	9.3	14.1	28.1	13.5	8.5	7.0	6.1	3.5	0.0	6.9	17.4	14.5	16.3	7.2	14.3
	CDR®+NACC-FTLD global score ≥ 1	18.0	25.3	37.5	22.3	14.8	13.1	12.5	7.7	4.2	12.7	30.4	30.2	24.9	12.4	22.1
p-value	CDR®+NACC-FTLD global score = 0	***<0.0005***	***<0.0005***	***<0.0005***	***<0.0005***	***<0.0005***	***<0.0005***	***<0.0005***	***0.018***	0.092	***<0.0005***	***<0.0005***	***<0.0005***	***<0.0005***	***<0.0005***	***<0.0005***
	CDR®+NACC-FTLD global score = 0.5	***<0.0005***	***<0.0005***	***<0.0005***	***<0.0005***	***<0.0005***	***<0.0005***	***0.001***	0.076	0.103	***<0.0005***	***<0.0005***	***<0.0005***	***<0.0005***	***0.015***	***<0.0005***
	CDR®+NACC-FTLD global score ≥ 1	***<0.0005***	***<0.0005***	***<0.0005***	***<0.0005***	***<0.0005***	***<0.0005***	***<0.0005***	***0.004***	***0.003***	***<0.0005***	***<0.0005***	***<0.0005***	***<0.0005***	***0.011***	***<0.0005***
MAPT		Whole	AV	LD	LP	VA	VLa	VLp	VPL	VM	Int	Mid	MD	LGN	MGN	Pul
CDR®+NACC-FTLD global score = 0	Mean	0.83	0.02	0.00	0.02	0.06	0.08	0.11	0.11	0.00	0.05	0.00	0.13	0.02	0.02	0.21
	SD	0.08	0.00	0.00	0.00	0.01	0.01	0.01	0.01	0.00	0.01	0.00	0.02	0.00	0.00	0.02
CDR®+NACC-FTLD global score = 0.5	Mean	0.80	0.02	0.00	0.02	0.05	0.08	0.10	0.10	0.00	0.05	0.00	0.13	0.02	0.02	0.21
	SD	0.08	0.00	0.00	0.00	0.01	0.01	0.01	0.01	0.00	0.01	0.00	0.02	0.00	0.00	0.02
CDR®+NACC-FTLD global score ≥ 1	Mean	0.69	0.01	0.00	0.01	0.05	0.07	0.09	0.09	0.00	0.04	0.00	0.10	0.02	0.01	0.18
	SD	0.10	0.00	0.00	0.00	0.01	0.01	0.01	0.01	0.00	0.01	0.00	0.02	0.00	0.00	0.02
% difference	CDR®+NACC-FTLD global score = 0	-1.6	-2.9	0.0	-1.4	-3.3	-2.7	-2.2	0.3	0.0	0.0	0.0	-3.7	0.5	-0.7	-0.8
	CDR®+NACC-FTLD global score = 0.5	1.6	-3.5	-18.8	-8.1	4.3	3.5	2.8	2.3	4.2	-1.2	0.0	0.9	-0.5	-0.7	-3.2
	CDR®+NACC-FTLD global score ≥ 1	15.3	15.9	25.0	14.2	13.9	13.5	14.1	13.0	12.5	13.5	21.7	26.4	12.2	16.3	12.3
p-value	CDR®+NACC-FTLD global score = 0	0.764	0.383	0.943	0.616	0.326	0.440	0.667	0.450	0.574	0.407	0.714	0.569	0.055	0.441	0.277
	CDR®+NACC-FTLD global score = 0.5	0.107	0.494	***0.011***	0.059	0.061	0.068	0.085	0.107	0.057	0.694	0.973	0.253	0.675	0.500	0.525
	CDR®+NACC-FTLD global score ≥ 1	***<0.0005***	***<0.0005***	***<0.0005***	***<0.0005***	***<0.0005***	***<0.0005***	***<0.0005***	***<0.0005***	***<0.0005***	***<0.0005***	***<0.0005***	***<0.0005***	0.093	***0.001***	***<0.0005***
GRN		Whole	AV	LD	LP	VA	VLa	VLp	VPL	VM	Int	Mid	MD	LGN	MGN	Pul
CDR®+NACC-FTLD global score = 0	Mean	0.81	0.02	0.00	0.01	0.06	0.08	0.10	0.10	0.00	0.05	0.00	0.13	0.02	0.02	0.21
	SD	0.08	0.00	0.00	0.00	0.01	0.01	0.01	0.01	0.00	0.01	0.00	0.02	0.00	0.00	0.02
CDR®+NACC-FTLD global score = 0.5	Mean	0.78	0.02	0.00	0.01	0.05	0.08	0.10	0.10	0.00	0.05	0.00	0.12	0.02	0.02	0.20
	SD	0.08	0.00	0.00	0.00	0.01	0.01	0.01	0.01	0.00	0.01	0.00	0.02	0.00	0.00	0.02
CDR®+NACC-FTLD global score ≥ 1	Mean	0.68	0.01	0.00	0.01	0.05	0.07	0.09	0.10	0.00	0.04	0.00	0.09	0.02	0.01	0.18
	SD	0.09	0.00	0.00	0.00	0.01	0.01	0.01	0.01	0.00	0.00	0.00	0.02	0.00	0.00	0.03
% difference	CDR®+NACC-FTLD global score = 0	-0.1	-0.6	3.1	-0.7	-0.5	-0.2	0.1	1.1	0.0	0.2	0.0	-0.1	-0.5	-0.7	0.2
	CDR®+NACC-FTLD global score = 0.5	4.3	4.7	9.4	2.7	2.7	1.7	2.0	1.9	0.0	1.0	8.7	8.8	0.9	2.0	2.2
	CDR®+NACC-FTLD global score ≥ 1	17.0	20.6	25.0	17.6	18.4	13.7	12.9	10.0	8.3	11.1	30.4	30.7	12.2	11.8	11.8
p-value	CDR®+NACC-FTLD global score = 0	0.796	0.877	0.539	0.872	0.813	0.823	0.580	0.146	0.123	0.598	0.446	0.672	0.586	0.921	0.318
	CDR®+NACC-FTLD global score = 0.5	0.362	0.268	0.289	0.516	0.892	0.731	0.848	0.989	0.931	0.518	0.559	0.036	0.125	0.534	0.407
	CDR®+NACC-FTLD global score ≥ 1	***<0.0005***	***<0.0005***	***<0.0005***	***<0.0005***	***<0.0005***	***<0.0005***	***<0.0005***	***<0.0005***	***0.004***	***<0.0005***	***<0.0005***	***<0.0005***	0.450	0.042	***0.001***

Groups		Whole	ai	as	i-tub	s-tub	pos
		Hypothalamus					
non-carriers	Mean	0.06	0.00	0.00	0.02	0.02	0.02
	SD	0.00	0.00	0.00	0.00	0.00	0.00
C9orf72		Whole	ai	as	i-tub	s-tub	pos
CDR®+NACC-FTLD global score = 0	Mean	0.06	0.00	0.00	0.02	0.02	0.02
	SD	0.01	0.00	0.00	0.00	0.00	0.00
CDR®+NACC-FTLD global score = 0.5	Mean	0.06	0.00	0.00	0.02	0.02	0.02
	SD	0.00	0.00	0.00	0.00	0.00	0.00
CDR®+NACC-FTLD global score ≥ 1	Mean	0.05	0.00	0.00	0.02	0.01	0.01
	SD	0.01	0.00	0.00	0.00	0.00	0.00
% difference	CDR®+NACC-FTLD global score = 0	-0.4	-2.6	0.3	-0.6	1.3	-1.5
	CDR®+NACC-FTLD global score = 0.5	3.0	-6.2	6.9	2.3	5.0	2.2
	CDR®+NACC-FTLD global score ≥ 1	11.3	19.8	24.8	0.0	14.3	16.7
p-value	CDR®+NACC-FTLD global score = 0	0.215	0.596	0.207	0.681	***0.008***	0.954
	CDR®+NACC-FTLD global score = 0.5	0.042	0.089	***0.017***	0.142	***0.016***	0.308
	CDR®+NACC-FTLD global score ≥ 1	***<0.0005***	***<0.0005***	***<0.0005***	0.311	***<0.0005***	***<0.0005***
MAPT		Whole	ai	as	i-tub	s-tub	pos
CDR®+NACC-FTLD global score = 0	Mean	0.06	0.00	0.00	0.02	0.02	0.02
	SD	0.01	0.00	0.00	0.00	0.00	0.00
CDR®+NACC-FTLD global score = 0.5	Mean	0.06	0.00	0.00	0.02	0.02	0.02
	SD	0.00	0.00	0.00	0.00	0.00	0.00
CDR®+NACC-FTLD global score ≥ 1	Mean	0.05	0.00	0.00	0.02	0.01	0.01
	SD	0.01	0.00	0.00	0.00	0.00	0.00
% difference	CDR®+NACC-FTLD global score = 0	0.5	4.4	1.2	-0.9	1.7	0.1
	CDR®+NACC-FTLD global score = 0.5	1.9	1.8	2.8	2.1	4.0	-0.5
	CDR®+NACC-FTLD global score ≥ 1	22.4	29.4	35.8	9.3	25.7	29.5
p-value	CDR®+NACC-FTLD global score = 0	0.269	0.164	0.388	0.607	0.047	0.544
	CDR®+NACC-FTLD global score = 0.5	0.047	0.376	0.130	0.086	0.044	0.529
	CDR®+NACC-FTLD global score ≥ 1	***<0.0005***	***<0.0005***	***<0.0005***	***<0.0005***	***<0.0005***	***<0.0005***
GRN		Whole	ai	as	i-tub	s-tub	pos
CDR®+NACC-FTLD global score = 0	Mean	0.06	0.00	0.00	0.02	0.02	0.02
	SD	0.01	0.00	0.00	0.00	0.00	0.00
CDR®+NACC-FTLD global score = 0.5	Mean	0.06	0.00	0.00	0.02	0.02	0.02
	SD	0.01	0.00	0.00	0.00	0.00	0.00
CDR®+NACC-FTLD global score ≥ 1	Mean	0.05	0.00	0.00	0.02	0.01	0.01
	SD	0.01	0.00	0.00	0.00	0.00	0.00
% difference	CDR®+NACC-FTLD global score = 0	0.5	0.1	0.9	0.9	0.7	-0.1
	CDR®+NACC-FTLD global score = 0.5	4.2	6.4	6.7	3.1	4.9	3.7
	CDR®+NACC-FTLD global score ≥ 1	13.5	22.3	25.0	-0.1	14.9	23.3
p-value	CDR®+NACC-FTLD global score = 0	0.143	0.686	0.236	0.137	0.156	0.687
	CDR®+NACC-FTLD global score = 0.5	0.048	0.237	0.072	0.129	0.058	0.450
	CDR®+NACC-FTLD global score ≥ 1	***<0.0005***	***<0.0005***	***<0.0005***	0.930	***<0.0005***	***<0.0005***

Groups		Whole	Vermis	I-IV	V	VI	VIIa-CrusI	VIIa-CrusII	VIIb	VIIIa	VIIIb	IX	X	DN	IN	FN
		Cerebellum														
non-carriers	Mean	7.36	0.33	0.43	0.63	1.12	1.41	1.18	0.52	0.53	0.49	0.39	0.06	0.23	0.03	0.00
	SD	0.62	0.03	0.05	0.07	0.12	0.18	0.15	0.06	0.05	0.06	0.07	0.01	0.03	0.00	0.00
C9orf72		Whole	Vermis	I-IV	V	VI	VIIa-CrusI	VIIa-CrusII	VIIb	VIIIa	VIIIb	IX	X	DN	IN	FN
CDR®+NACC-FTLD global score = 0	Mean	7.26	0.32	0.42	0.62	1.10	1.39	1.16	0.51	0.53	0.49	0.39	0.06	0.23	0.03	0.00
	SD	0.60	0.03	0.05	0.07	0.12	0.19	0.18	0.06	0.05	0.05	0.06	0.01	0.02	0.00	0.00
CDR®+NACC-FTLD global score = 0.5	Mean	7.19	0.33	0.42	0.61	1.08	1.36	1.17	0.51	0.52	0.47	0.39	0.06	0.24	0.03	0.00
	SD	0.69	0.04	0.05	0.08	0.12	0.20	0.17	0.06	0.05	0.06	0.07	0.01	0.03	0.00	0.00
CDR®+NACC-FTLD global score ≥ 1	Mean	6.60	0.30	0.41	0.59	0.99	1.27	1.03	0.46	0.48	0.42	0.34	0.06	0.22	0.03	0.00
	SD	0.69	0.04	0.05	0.07	0.11	0.17	0.19	0.08	0.07	0.07	0.06	0.01	0.03	0.00	0.00
% difference	CDR®+NACC-FTLD global score = 0	1.3	0.3	1.5	1.1	1.4	1.7	2.3	2.5	0.9	0.3	-0.4	-2.2	0.1	-2.6	-5.3
	CDR®+NACC-FTLD global score = 0.5	2.3	-1.9	2.3	3.1	3.4	3.4	1.3	2.3	2.5	3.4	1.4	0.9	-1.5	-4.4	-5.3
	CDR®+NACC-FTLD global score ≥ 1	10.3	6.5	5.5	5.9	11.9	9.9	12.9	11.6	10.4	14.0	12.5	2.4	7.4	5.1	0.0
p-value	CDR®+NACC-FTLD global score = 0	***0.006***	0.359	0.076	0.068	0.014	0.046	***0.011***	***0.009***	0.183	0.390	0.649	0.150	0.291	0.197	0.141
	CDR®+NACC-FTLD global score = 0.5	0.189	0.330	0.337	0.176	0.153	0.231	0.605	0.316	0.245	0.137	0.901	0.451	0.518	0.105	0.366
	CDR®+NACC-FTLD global score ≥ 1	***<0.0005***	***0.007***	0.145	0.306	***0.001***	0.023	***<0.0005***	***<0.0005***	***<0.0005***	***<0.0005***	0.026	0.186	***0.005***	0.484	0.533
MAPT		Whole	Vermis	I-IV	V	VI	VIIa-CrusI	VIIa-CrusII	VIIb	VIIIa	VIIIb	IX	X	DN	IN	FN
CDR®+NACC-FTLD global score = 0	Mean	7.62	0.33	0.44	0.64	1.16	1.50	1.24	0.53	0.54	0.49	0.41	0.06	0.24	0.03	0.00
	SD	0.62	0.03	0.03	0.06	0.14	0.17	0.17	0.05	0.05	0.06	0.07	0.01	0.03	0.00	0.00
CDR®+NACC-FTLD global score = 0.5	Mean	7.79	0.34	0.43	0.66	1.19	1.55	1.26	0.54	0.55	0.50	0.41	0.06	0.25	0.03	0.00
	SD	0.63	0.04	0.04	0.05	0.15	0.20	0.21	0.05	0.04	0.05	0.07	0.01	0.03	0.00	0.00
CDR®+NACC-FTLD global score ≥ 1	Mean	7.08	0.33	0.41	0.60	1.04	1.33	1.14	0.51	0.53	0.48	0.39	0.06	0.23	0.03	0.00
	SD	0.58	0.04	0.04	0.07	0.10	0.17	0.15	0.06	0.05	0.07	0.06	0.01	0.02	0.00	0.00
% difference	CDR®+NACC-FTLD global score = 0	-3.5	-2.0	-1.9	-2.4	-3.9	-6.5	-4.8	-1.7	-0.7	0.3	-6.0	-1.4	-0.9	-1.5	0.0
	CDR®+NACC-FTLD global score = 0.5	-5.8	-5.3	0.6	-5.4	-6.6	-10.0	-6.5	-3.6	-3.1	-2.0	-4.1	-4.8	-8.1	-10.6	-7.9
	CDR®+NACC-FTLD global score ≥ 1	3.8	-2.2	4.5	5.0	7.3	5.6	3.5	1.4	0.5	2.1	1.1	-2.4	3.2	3.3	0.0
p-value	CDR®+NACC-FTLD global score = 0	0.088	0.376	0.437	0.474	0.339	0.016	0.102	0.718	0.985	0.485	0.221	0.277	0.850	0.741	0.965
	CDR®+NACC-FTLD global score = 0.5	0.108	0.295	0.492	0.278	0.124	0.035	0.411	0.536	0.439	0.836	0.623	0.664	0.192	0.037	0.323
	CDR®+NACC-FTLD global score ≥ 1	0.946	0.140	0.291	0.498	0.482	0.774	0.815	0.747	0.835	0.974	0.216	0.439	0.486	0.929	0.926
GRN		Whole	Vermis	I-IV	V	VI	VIIa-CrusI	VIIa-CrusII	VIIb	VIIIa	VIIIb	IX	X	DN	IN	FN
CDR®+NACC-FTLD global score = 0	Mean	7.34	0.33	0.42	0.62	1.11	1.41	1.19	0.52	0.53	0.49	0.39	0.06	0.23	0.03	0.00
	SD	0.64	0.03	0.04	0.06	0.12	0.18	0.16	0.06	0.06	0.07	0.07	0.01	0.03	0.00	0.00
CDR®+NACC-FTLD global score = 0.5	Mean	7.00	0.32	0.41	0.60	1.04	1.32	1.14	0.50	0.51	0.47	0.38	0.06	0.23	0.03	0.00
	SD	0.52	0.04	0.04	0.06	0.13	0.15	0.13	0.05	0.05	0.05	0.05	0.01	0.03	0.00	0.00
CDR®+NACC-FTLD global score ≥ 1	Mean	6.75	0.31	0.43	0.61	1.03	1.26	1.03	0.47	0.49	0.45	0.37	0.06	0.23	0.03	0.00
	SD	0.71	0.04	0.04	0.06	0.13	0.19	0.17	0.06	0.06	0.07	0.07	0.01	0.03	0.00	0.00
% difference	CDR®+NACC-FTLD global score = 0	0.3	-0.3	1.8	1.3	1.2	0.0	-0.2	-0.1	0.3	-0.4	-0.9	-0.2	-0.4	-1.8	-2.6
	CDR®+NACC-FTLD global score = 0.5	4.9	2.7	4.5	4.3	7.0	6.8	4.1	3.6	4.3	4.6	2.9	0.9	2.1	-1.8	0.0
	CDR®+NACC-FTLD global score ≥ 1	8.3	3.6	1.4	3.6	8.5	10.6	13.0	10.6	7.9	7.7	6.5	-0.5	3.6	2.6	-2.6
p-value	CDR®+NACC-FTLD global score = 0	0.317	0.761	0.058	0.103	0.076	0.610	0.715	0.935	0.576	0.997	0.840	0.894	0.866	0.351	0.260
	CDR®+NACC-FTLD global score = 0.5	0.064	0.416	0.100	0.230	0.027	0.065	0.577	0.370	0.102	0.205	0.969	0.766	0.899	0.118	0.931
	CDR®+NACC-FTLD global score ≥ 1	***0.001***	0.242	0.882	0.907	0.146	0.006	***<0.0005***	***<0.0005***	***0.001***	0.108	0.992	0.922	0.405	0.905	0.488

Groups		Whole	SCP	MB	Pons	ME
		Brainstem				
non-carriers	Mean	1.83	0.02	0.43	1.02	0.36
	SD	0.16	0.00	0.03	0.10	0.04
C9orf72		Whole	SCP	MB	Pons	ME
CDR®+NACC-FTLD global score = 0	Mean	1.88	0.02	0.44	1.05	0.37
	SD	0.15	0.00	0.04	0.10	0.03
CDR®+NACC-FTLD global score = 0.5	Mean	1.86	0.02	0.43	1.04	0.37
	SD	0.18	0.00	0.03	0.12	0.03
CDR®+NACC-FTLD global score ≥ 1	Mean	1.76	0.02	0.41	0.99	0.35
	SD	0.22	0.00	0.06	0.13	0.04
% difference	CDR®+NACC-FTLD global score = 0	-3.2	-1.2	-3.3	-2.8	-4.4
	CDR®+NACC-FTLD global score = 0.5	-2.0	2.9	-1.4	-1.9	-3.5
	CDR®+NACC-FTLD global score ≥ 1	3.7	-1.7	5.2	3.4	2.6
p-value	CDR®+NACC-FTLD global score = 0	0.012	0.547	0.011	0.048	***0.001***
	CDR®+NACC-FTLD global score = 0.5	0.255	0.803	0.289	0.341	0.157
	CDR®+NACC-FTLD global score ≥ 1	0.065	0.996	0.016	0.094	0.270
MAPT		Whole	SCP	MB	Pons	ME
CDR®+NACC-FTLD global score = 0	Mean	1.85	0.02	0.43	1.04	0.36
	SD	0.16	0.00	0.04	0.11	0.04
CDR®+NACC-FTLD global score = 0.5	Mean	1.89	0.02	0.44	1.05	0.38
	SD	0.21	0.00	0.05	0.12	0.05
CDR®+NACC-FTLD global score ≥ 1	Mean	1.72	0.02	0.39	0.98	0.34
	SD	0.16	0.00	0.04	0.10	0.03
% difference	CDR®+NACC-FTLD global score = 0	-1.4	-0.6	-0.7	-1.8	-1.1
	CDR®+NACC-FTLD global score = 0.5	-3.5	2.9	-3.4	-2.9	-5.7
	CDR®+NACC-FTLD global score ≥ 1	5.7	8.7	9.2	4.5	4.8
p-value	CDR®+NACC-FTLD global score = 0	0.444	0.709	0.852	0.388	0.473
	CDR®+NACC-FTLD global score = 0.5	0.506	0.594	0.572	0.569	0.400
	CDR®+NACC-FTLD global score ≥ 1	0.012	0.011	***<0.0005***	0.075	0.122
GRN		Whole	SCP	MB	Pons	ME
CDR®+NACC-FTLD global score = 0	Mean	1.84	0.02	0.43	1.03	0.36
	SD	0.15	0.00	0.03	0.09	0.04
CDR®+NACC-FTLD global score = 0.5	Mean	1.84	0.02	0.44	1.03	0.36
	SD	0.15	0.00	0.03	0.09	0.04
CDR®+NACC-FTLD global score ≥ 1	Mean	1.71	0.02	0.39	0.95	0.34
	SD	0.17	0.00	0.03	0.10	0.04
% difference	CDR®+NACC-FTLD global score = 0	-0.5	2.3	-0.9	-0.3	-1.0
	CDR®+NACC-FTLD global score = 0.5	-0.8	5.8	-1.6	-0.5	-0.8
	CDR®+NACC-FTLD global score ≥ 1	6.6	5.2	8.3	6.9	3.7
p-value	CDR®+NACC-FTLD global score = 0	0.679	0.237	0.347	0.869	0.554
	CDR®+NACC-FTLD global score = 0.5	0.342	0.105	0.070	0.552	0.328
	CDR®+NACC-FTLD global score ≥ 1	***<0.0005***	***0.011***	***<0.0005***	***<0.0005***	0.169

Supplementary Figure 1. Plots representing the means and standard error bars for the whole brain volumes for each of the stages in *C9orf72*, *MAPT* and *GRN* mutation carriers. Volumes as expressed as % the mean volumes in controls. * indicates a significant difference from controls after correcting for multiple comparisons.

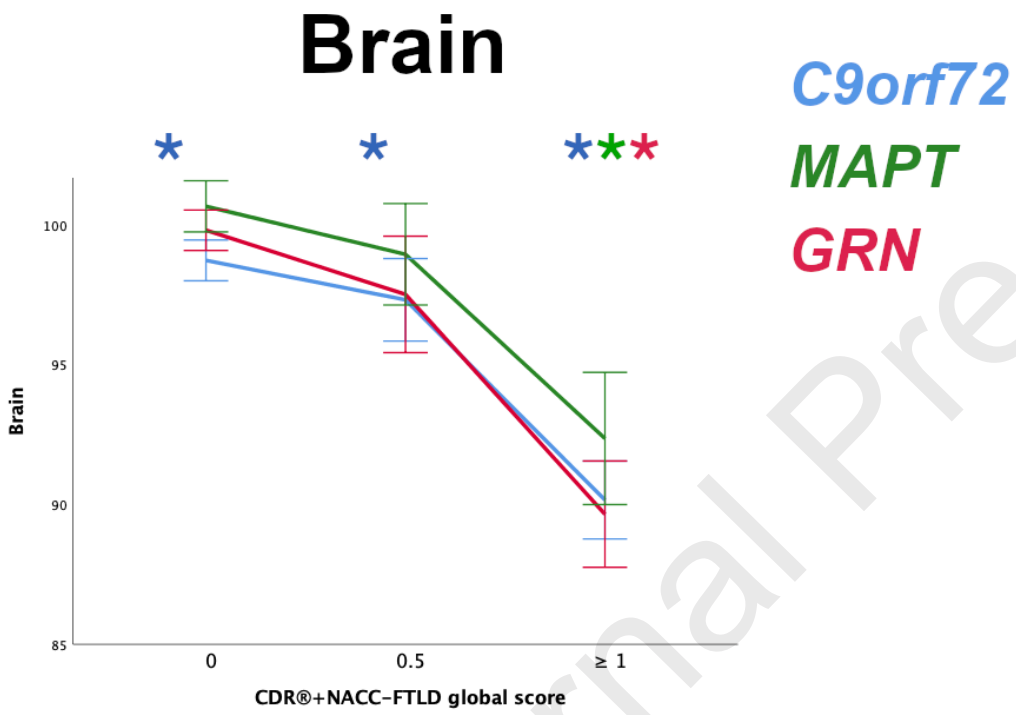

Supplementary Figure 2. Plots representing the means and standard error bars for the cortical regions for each of the stages in *C9orf72*, *MAPT* and *GRN* mutation carriers. Volumes as expressed as % the mean volumes in controls. * indicates a significant difference from controls after correcting for multiple comparisons.

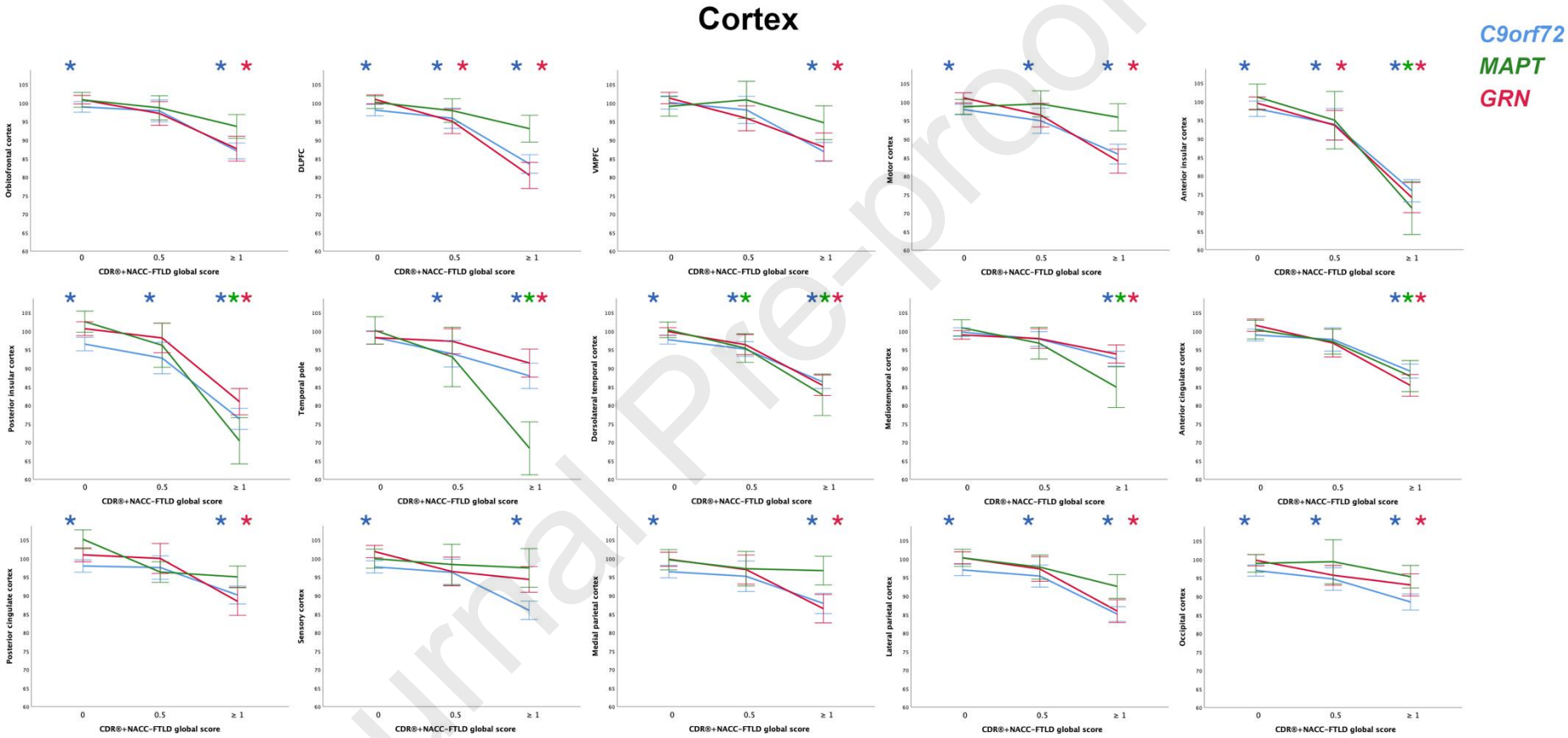

Credit Author Statement

MB drafted the initial version of the manuscript and the figures and performed the analysis. JDR contributed to the study design and is the Principal Investigator of the GENetic Frontotemporal Initiative study. All authors contributed to the acquisition of data, to the study coordination, to the interpretation of data, and they all revised the manuscript.

Highlights

- Progressive and differential atrophy pattern at presymptomatic stages across genes
- Early presymptomatic brain changes detectable only by looking at small regions
- *C9orf72* shows the earliest and most widespread changes (cortex, pulvinar, cerebellum)
- *MAPT* shows early differences in the dorsolateral temporal, amygdala and hippocampus
- Late presymptomatic changes in *GRN* in dorsolateral prefrontal, insula, presubiculum

Cortex

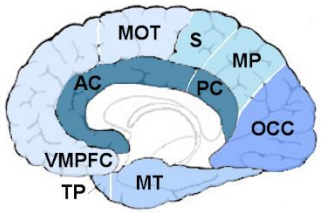

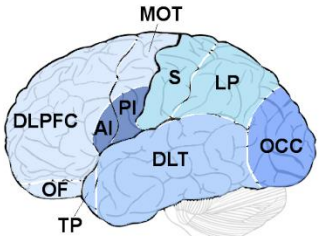

Basal ganglia and Basal forebrain

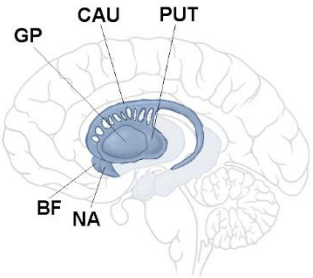

Brainstem and Cerebellum

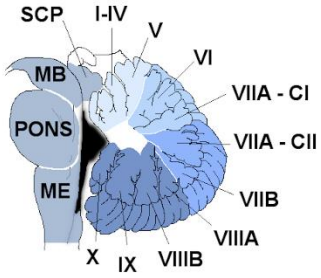

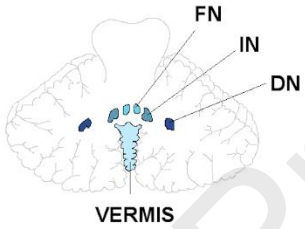

Amygdala

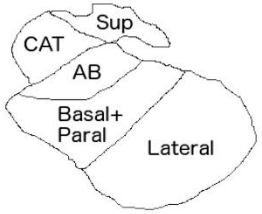

Hippocampus

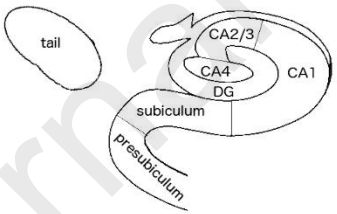

Thalamus

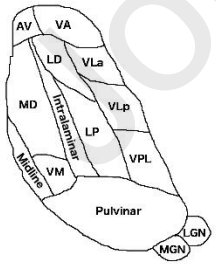

Hypothalamus